Threshold pion photo-production off nucleons using the nuclear model with explicit pions

Martin Mikkelsen
201706771

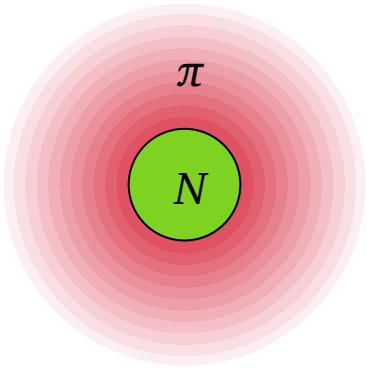

Master's thesis
Supervisor: Dmitri Fedorov

Department of Physics and Astronomy
Aarhus University
Denmark

November 2022

Summary

This is a bachelor's project about relativistic kinematics. This means a theoretical description of particle's motion without considering the forces that cause them to move, in the relativistic limit. More specifically this project illuminates three-particle decays with kinematic invariant quantities. The theory introduces an approach to examine an anomaly that occurred in an experiment when a Hungarian research team measured transitions in ^{8}Be. It combines considerations of phase space for three-particle decay with resonance amplitudes and angular distributions. This leads to experimental predictions separated into three parts depending on the spin state of the resonant particle, the X17 particle. This project concludes that the formalism is consistent with the relativistic scattering angles in the laboratory system and how experimental results can be illustrated using kinematic invariants. Three angles are proposed to investigate the X17 particle experimentally.

Resumé

Dette bachelorprojekt omhandler relativistisk kinematisk. Det vil altså sige en teoretisk beskrivelse af partiklers bevægelse uden ydre påvirkning i den relativistiske grænse. Mere specifikt belyser dette projekt 3-partikel henfald ved hjælp af kinematiske invariante størrelser. Teorien i projektet introducerer den tilgang, der er anvendt til at undersøge en anormalitet i et forsøg, som opstod da et ungarnsk forskerhold målte overgange i ^{8}Be. Teorien kombinerer overvejelser omkring faserum for tre-partikel henfald med resonansamplituder og vinkelfordelinger. Dette fører til eksperimentelle forudsigelser, der er inddelt i tre dele afhængig af spintilstanden for resonanspartiklen, X17. Projektet konkluderer, at formalismen er konsistent med den relativistiske spredningsvinkel i laboratoriets hvileramme og viser hvordan eksperimentelle resultater kan repræsenteres ved kinematiske invariante størrelser. Der foreslås tre vinkler, som kan måles eksperimentelt for at undersøge X17 partiklen.

Colophon

Threshold pion photo-production off nucleons using the nuclear model with explicit pions

Master's thesis by Martin Mikkelsen

The project is supervised by Dmitri Fedorov

Typeset by the author using LaTeX and the memoir document class. Figures are made with the using the Seaborn package in Python and the Tikz package.

Code for document, figures and numerical calculations can be found on `https://github.com/MartinMikkelsen`

Printed at Aarhus University

Contents

Chapter 1

Introduction

Lorem ipsum dolor sit amet, consectetuer adipiscing elit. Ut purus elit, vestibulum ut, placerat ac, adipiscing vitae, felis. Curabitur dictum gravida mauris. Nam arcu libero, nonummy eget, consectetuer id, vulputate a, magna. Donec vehicula augue eu neque. Pellentesque habitant morbi tristique senectus et netus et malesuada fames ac turpis egestas. Mauris ut leo. Cras viverra metus rhoncus sem. Nulla et lectus vestibulum urna fringilla ultrices. Phasellus eu tellus sit amet tortor gravida placerat. Integer sapien est, iaculis in, pretium quis, viverra ac, nunc. Praesent eget sem vel leo ultrices bibendum. Aenean faucibus. Morbi dolor nulla, malesuada eu, pulvinar at, mollis ac, nulla. Curabitur auctor semper nulla. Donec varius orci eget risus. Duis nibh mi, congue eu, accumsan eleifend, sagittis quis, diam. Duis eget orci sit amet orci dignissim rutrum.

Nam dui ligula, fringilla a, euismod sodales, sollicitudin vel, wisi. Morbi auctor lorem non justo. Nam lacus libero, pretium at, lobortis vitae, ultricies et, tellus. Donec aliquet, tortor sed accumsan bibendum, erat ligula aliquet magna, vitae ornare odio metus a mi. Morbi ac orci et nisl hendrerit mollis. Suspendisse ut massa. Cras nec ante. Pellentesque a nulla. Cum sociis natoque penatibus et magnis dis parturient montes, nascetur ridiculus mus. Aliquam tincidunt urna. Nulla ullamcorper vestibulum turpis. Pellentesque cursus luctus mauris.

1.1 Units

We will work in "God-given" units where

$$\hbar = c = 1. \tag{1.1}$$

Discussions of spin and isospin make use of the Pauli spin matrices

$$\sigma_1 = \begin{pmatrix} 0 & 1 \\ 1 & 0 \end{pmatrix}, \quad \sigma_2 = \begin{pmatrix} 0 & -i \\ i & 0 \end{pmatrix}, \quad \sigma_3 = \begin{pmatrix} 1 & 0 \\ 0 & 1 \end{pmatrix}, \tag{1.2}$$

which also defines the Pauli vector given by

$$\boldsymbol{\sigma} = \sigma_1 \hat{x}_1 + \sigma_2 \hat{x}_2 + \sigma_3 \hat{x}_3, \tag{1.3}$$

and analogously for the isospin vector. The two level system of the nucleon has the following representation

$$|p\rangle = \begin{pmatrix} 1 \\ 0 \end{pmatrix}, \quad |n\rangle = \begin{pmatrix} 0 \\ 1 \end{pmatrix}, \tag{1.4}$$

Chapter 2

Theoretical background

Chapter 3

The model

We consider a nuclear model where the nucleus is held together by emitting and absorbing mesons, and the mesons are treated explicitly [Fedorov 2020]. We are considering the regime of low-energy nuclear physics and this model is different from conventional interaction models in several ways. Firstly, the nucleons interact by emitting and absorbing mesons and not via a phenomenological potential. Conceptually this is similar to the one-boson-exchange model. Secondly, the number of parameters is greatly reduced. Regardless of the meson type, the number of parameters is two; the range and the strength of the meson-nucleon coupling are denoted b and S respectively. In the case of the pion, the central force, tensor force and the three-body force are all concealed within these two parameters. This model should be able to reproduce phenomena within the realm of low-energy nuclear physics such as the deuteron, nucleon-nucleon scattering, pion-nucleon scattering and pion photoproduction. The low energy regime also enables the use of the Schödinger equation to describe the equations of motion. The model must be constructed in a way such that usual quantum numbers are conserved; this means conservation of isospin, angular momentum and parity.

3.1 Nuclear interacting model with explicit pions

In the following, we focus on the nuclear model with explicit pions. The pion is the lightest of the strongly interacting particles with a mass of about 15% of the nucleon mass. This yields a large Compton wavelength of 1.4 fm which means the longest contribution to nucleon-nucleon interactions. Furthermore, the pion is a significant component of the nuclear wave function where the pion dominates meson exchange corrections to different nuclear properties. In general, the bare nucleon is surrounded by several virtual pions. They are virtual in the same sense that the positron-electron pair are virtual in pair creation from a photon. It is important to stress the fact that these are virtual since they can have properties possible for true particles. The multi-component wave function of the nucleon can be written as

$$\Psi_N = \begin{bmatrix} \psi_N \\ \psi_{N\pi} \\ \psi_{N\pi\pi} \\ \vdots \end{bmatrix}, \tag{3.1}$$

where ψ_N is the bare nucleon and the other wave functions are dressed by an arbitrary number of pions indicated by the subscripts. Assuming

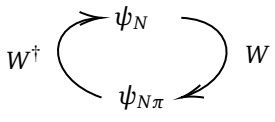

Figure 3.1: Illustration of the pion-nucleon operator, W

the nuclear interaction conserved isospin, angular momentum and parity we can construct the following operator for the pion-nucleon operator

$$W \equiv (\boldsymbol{\tau} \cdot \boldsymbol{\pi})(\boldsymbol{\sigma} \cdot \mathbf{r}) f(r) \tag{3.2}$$

$$W^\dagger \equiv \int_V \mathrm{d}^3 r \, (\boldsymbol{\tau} \cdot \boldsymbol{\pi})^\dagger (\boldsymbol{\sigma} \cdot \mathbf{r})^\dagger f(r), \tag{3.3}$$

where $\boldsymbol{\tau}$ is the isovector of Pauli matrices acting on the nucleon in isospin space and $\boldsymbol{\sigma}$ is the same but for spin space and $\mathbf{r}$ is the relative coordinate distance between the nucleon and the pion. These operators ensure the conservation of isospin, angular momentum and parity. The isovector of pions is denoted $\boldsymbol{\pi}$ and can be combined with $\boldsymbol{\tau}$ can be represented as a traceless 2-by-2 hermitian matrix given by

$$\boldsymbol{\tau} \cdot \boldsymbol{\pi} = \tau_0 \pi_0 + \sqrt{2}\tau_- \pi^+ \sqrt{2}\tau_+ \pi^- = \begin{bmatrix} \pi^0 & \sqrt{2}\pi^- \\ \sqrt{2}\pi^+ & -\pi^0 \end{bmatrix}, \tag{3.4}$$

where the isospin coefficients will be important later when we discuss different photoproduction processes. Similarly, by expanding the matrices in spin space and using the spherical tensor operator we get the following matrix in terms of the spherical harmonics

$$\boldsymbol{\sigma} \cdot \mathbf{r} = \sqrt{\frac{4\pi}{3}} r \begin{bmatrix} Y_1^0 & \sqrt{2}Y_1^{-1} \\ \sqrt{2}Y_1^1 & Y_1^0 \end{bmatrix}, \tag{3.5}$$

where similar to in isospin space, the off-diagonals include a factor $\sqrt{2}$.

There is also a phenomenological, short-range form factor $f(r)$ given by

$$f(r) = \frac{S}{b} \mathrm{e}^{-r^2/b^2}, \tag{3.6}$$

where S and b are the pion-nucleon coupling strength and range respectively– these are illustrated in figure 3.2. The action of annihilating a pion must include the integral over coordinate space to remove the coordinate. We now have everything we need to construct a general Hamiltonian for the multi-component wave function of the nucleon in (3.1)

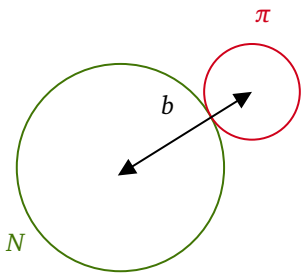

Figure 3.2: Schematic figure of the system to describe the form factor, (3.6). The pion is assumed to sit on the surface.

$$H = \begin{bmatrix} K_N & W^\dagger & 0 & \dots \\ W & K_N + K_\pi + m_\pi c^2 + V_C & W^\dagger & \dots \\ 0 & W & K_N + K_{\pi(1)} + K_{\pi(2)} + 2m_\pi c^2 + V_C & \dots \\ \vdots & \vdots & \vdots & \ddots \end{bmatrix}, \tag{3.7}$$

where the kinetic operators are given by

$$K_N = \frac{-\hbar^2}{2m_N c^2} \frac{\partial}{\partial \mathbf{R}^2} \tag{3.8}$$

$$K_\pi = \frac{-\hbar^2}{2m_\pi c^2} \frac{\partial}{\partial \mathbf{r}^2}. \tag{3.9}$$

Note the different derivatives– here $\mathbf{R}$ is the center-of-mass coordinate and $\mathbf{r}$ is the relative coordinate. The subscripts on the kinetic operators in (3.7) represent the order in which the pions are created. Should there be charged particles involved one must include a Coulomb interaction denoted by V_C. From (3.1) and (3.7) we can construct the general Schrödinger equation

$$H\Psi_N = E\Psi_N, \tag{3.10}$$

where the ground state is the bare nucleon surrounded by virtual pions. The ground state energy in the rest frame of the nucleon gives the mass of the physical nucleon. Within the framework of this model, one can generate a physical pion by supplying enough energy such that the pion is no longer virtual. The pion is trapped behind a potential barrier of height $m_\pi c^2 = 140$ MeV and cannot leave unless this or more energy is supplied to the system.

3.2 Dressing of the nucleon in the one pion approximation

We now consider the scenario where a photon interacts with the nucleon-pion systems and generates a physical pion. This means the energy is higher than the potential barrier also when taking recoil effects into account. This also hints how a pion photoproduction process would emerge naturally as a disintegration process in this nuclear model. To generate more pions the photon energy would have to be increased by the same amount. This also means one could assume the first pion is responsible for the largest contribution to the nucleon dressing. This will be referred to as the one pion approximation. As a proof-of-concept we constrain ourselves to the one pion approximation and adding more pions should in principle be straight forward extension of the following calculations.

Returning to (3.1) and enforcing the one pion approximation yields

$$\Psi = \begin{bmatrix} \psi_N(\mathbf{R}) \\ \psi_{N\pi}(\mathbf{r}) \end{bmatrix}. \tag{3.11}$$

The Hamiltonian which acts on the two-component wave function in (3.11) is given by[1]

$$H = \begin{bmatrix} K_N & W^\dagger \\ W & K_N + K_\pi + m_\pi c^2 \end{bmatrix}, \tag{3.12}$$

$$\psi_p = p \uparrow \frac{1}{\sqrt{V}}, \quad \psi_{N\pi} = (\boldsymbol{\tau} \cdot \boldsymbol{\pi})(\boldsymbol{\sigma} \cdot \mathbf{r})\phi(r) p \uparrow \frac{1}{\sqrt{V}}, \tag{3.13}$$

where V is the volume, $\boldsymbol{\tau}$ is combination of the matrices $\tau_{1,2,3}$ into a matrix vector–completely analogous to the vector $\boldsymbol{\sigma}$ of spin Pauli matrices. Also, we have chosen the proton as isospin up state in the nucleon

$$|p\rangle = \begin{bmatrix} 1 \\ 0 \end{bmatrix}. \tag{3.14}$$

From (3.13)

$$\Psi = \begin{bmatrix} \psi_p \\ \psi_{N\pi} \end{bmatrix}, \tag{3.15}$$

To construct a Hamiltonian we define two operators corresponding to creation and annihilation of the meson. We define the operator as

$$W \equiv (\boldsymbol{\tau} \cdot \boldsymbol{\pi})(\boldsymbol{\sigma} \cdot \mathbf{r}) f(r), \tag{3.16}$$

where $f(r)$ is some form factor given by where $S \simeq 10\,\text{MeV}$ and $b \simeq 1\,\text{fm}$. This is illustrated in figure 3.2. Note that (3.6) must have units of energy per length such that (3.16) has units of energy.

From (3.16) we can construct the Hamiltonian of the system

$$H \doteq \begin{bmatrix} K_{\mathbf{R}} & W^\dagger \\ W & K_{\mathbf{R}} + K_{\mathbf{r}} + m_\pi c^2 \end{bmatrix}, \tag{3.17}$$

1. Strictly speaking one should use a three-component wave function to account for the mass difference between π^0 and $\pi^\pm$. This is done in appendix C.

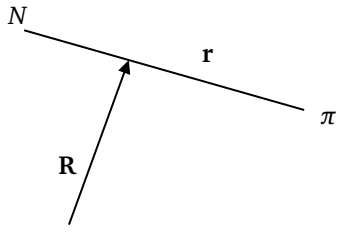

Figure 3.3: Absolute and relative distance.

where K_i represents the kinetic term of particle i. Also, R represents the absolute distance and r is the relative distance as illustrated in figure 3.3. Plugging this into the Schrödinger equation yields

$$\begin{bmatrix} K_{\mathbf{p}} & W^{\dagger} \\ W & K_{\mathbf{R}} + K_{\mathbf{r}} + m_{\pi}c^2 \end{bmatrix} \begin{bmatrix} \psi_p \\ \psi_{N\pi} \end{bmatrix} = E \begin{bmatrix} \psi_p \\ \psi_{N\pi} \end{bmatrix}. \tag{3.18}$$

Expanding (3.18) yields two equations

$$K_{\mathbf{p}}\psi_p + W^{\dagger}\psi_{N\pi} = E\psi_p \tag{3.19}$$

$$W\psi_p + (K_{\mathbf{R}} + K_{\mathbf{r}} + m_{\pi})\psi_{N\pi} = E\psi_{N\pi}. \tag{3.20}$$

The first term in (3.19) vanishes and inserting (3.16) yields

$$\int_V \mathrm{d}^3 r \, (\boldsymbol{\tau}\cdot\boldsymbol{\pi})^{\dagger}(\boldsymbol{\sigma}\cdot\mathbf{r})^{\dagger} f(r)\phi(r)(\boldsymbol{\tau}\cdot\boldsymbol{\pi})(\boldsymbol{\sigma}\cdot\mathbf{r})p\frac{1}{\sqrt{V}} = Ep\frac{1}{\sqrt{V}} \tag{3.21}$$

2. $(\boldsymbol{\tau}\cdot\boldsymbol{\pi})^{\dagger}(\boldsymbol{\tau}\cdot\boldsymbol{\pi}) = 3$ and $(\boldsymbol{\sigma}\cdot\mathbf{r})^{\dagger}(\boldsymbol{\sigma}\cdot\mathbf{r}) = r^2$

This can be further simplified using relations for the matrix vectors[2]

$$12\pi \int_0^{\infty} \mathrm{d}r \, f(r)\phi(r)r^4 = E. \tag{3.22}$$

Similarly for (3.20) where the term $K_{\mathbf{R}}\psi_{N\pi}$ vanishes,

$$(\boldsymbol{\tau}\cdot\boldsymbol{\pi})(\boldsymbol{\sigma}\cdot\mathbf{r})f(r)p\frac{1}{\sqrt{V}} - \frac{\hbar^2}{2\mu}\nabla_{\mathbf{r}}^2(\boldsymbol{\tau}\cdot\boldsymbol{\pi})(\boldsymbol{\sigma}\cdot\mathbf{r})p\frac{1}{\sqrt{V}}\phi(r) = (E - m_{\pi}c^2)(\boldsymbol{\tau}\cdot\boldsymbol{\pi})(\boldsymbol{\sigma}\cdot\mathbf{r})\phi(r)p\frac{1}{\sqrt{V}}, \tag{3.23}$$

where μ is the reduced mass of the system. This equation can be further simplified by using a vector operator relation[3]

3. $\nabla^2(\mathbf{r}\phi(r)) = \mathbf{r}\left(\frac{\mathrm{d}^2\phi(r)}{\mathrm{d}r^2} + \frac{4}{r}\frac{\mathrm{d}\phi(r)}{\mathrm{d}r}\right)$

$$f(r) - \frac{\hbar^2}{2\mu}\left(\frac{\mathrm{d}^2\phi(r)}{\mathrm{d}r^2} + \frac{4}{r}\frac{\mathrm{d}\phi(r)}{\mathrm{d}r}\right) = (E - m_{\pi}c^2)\phi(r). \tag{3.24}$$

This means equation (3.22) and (3.24) are the two equations that must be solved numerically.

$$\left.\begin{aligned} &12\pi \textstyle\int_0^{\infty} \mathrm{d}r \, f(r)\phi(r)r^4 = E \\ &f(r) - \tfrac{\hbar^2}{2\mu}\left(\tfrac{\mathrm{d}^2\phi(r)}{\mathrm{d}r^2} + \tfrac{4}{r}\tfrac{\mathrm{d}\phi(r)}{\mathrm{d}r}\right) + m_{\pi}c^2\phi(r) = E\phi(r) \end{aligned}\right\} \tag{3.25}$$

The bracket on the right is used to empathise that (3.25) is a coupled system.

3.2.1 Numerical considerations

To solve the system of equations (3.25) one can consider two different numerical approaches.

For a given E one can solve the second order corresponding to $\phi[E]$. Conversely, for a given $\phi(r)$ one can calculate the integral to find $E[\phi]$. This leads to the fixed-point equation given by

$$E[\phi[\mathcal{E}]] = \mathcal{E}, \tag{3.26}$$

which is a single variable non-linear equation. (3.26) can be solved using a root-finding algorithm.

The second approach consists of reformulating the system (3.25) as a boundary value problem with the following conditions

$$I'(r) = 12\pi f(r)\phi(r)r^4, \quad I(0) = 0, \, I(\infty) = E. \tag{3.27}$$

The equation starts from a singular point and extends to an infinite point. Considerations about how to scale the starting point and stopping point as a function of b are needed. These two points must be proportional to b with some arbitrary proportionality constant. In the regime of nuclear physics, we expect the wavefunction to extend up to a length within the order of magnitude of ten Fermi. Quantitatively this means a small constant of proportionality $O(0.01)$ in front of r_{min} and another constant $O(1)$ in front of r_{max}.

We require the solution to stay finite which means approximations are needed at both limits. At $r \to 0$ the differential equation is approximately an Euler-Cauchy equation with basis solutions 1 and r^{-1}. For finite solutions the latter is ignored which means $\phi'(a) = 0$ is the requirement for $a \approx 0$.[4] For $r \to \infty$ the dominating term is the differential equation are

$$-\phi''(r) + 2\mu(m_\pi c^2 - E)\phi(r) = 0. \tag{3.28}$$

Since we expect a negative value for E the basis solutions are $\exp\left\{\pm\sqrt{2\mu(m_\pi c^2 + |E|)}\right\}r$. In the case of a positive sign the solution diverges. For the basis solution with negative exponents we have

$$\phi'(r) + \sqrt{2\mu(m_\pi c^2 + |E|)}\phi(r) = 0. \tag{3.29}$$

These two conditions are suitable boundary conditions for the left and right boundaries, respectively. The solutions can be seen in figure 3.4.

4. You would end up with the same conclusion if you consider $\phi = a + r^n$ and plug this into $\phi'' + 4\phi'/r = 0$, which yields $n = 0, -1$.

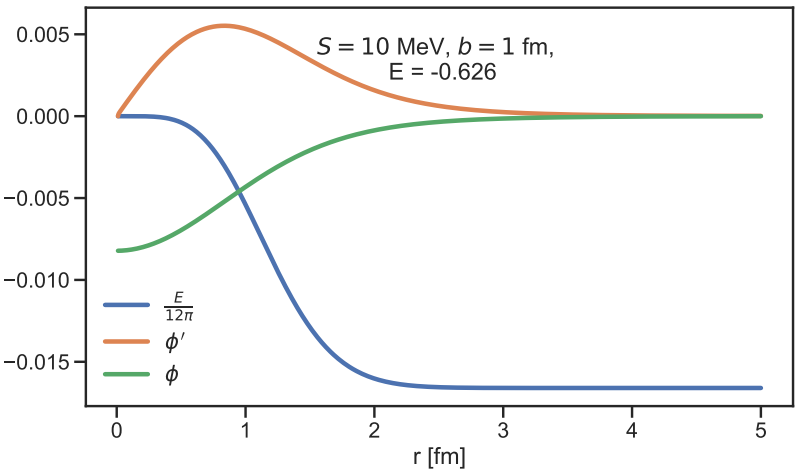

Figure 3.4: Boundary value problem solutions. The plot is generated using a tolerance of 10^{-6}. The RMS values of the relative residuals over each mesh intervals is shown in the Appendix. For clarity, I have scaled the energy.

The algorithm converges and a solution to (3.18) is found. Also, note that since we expect the energy to be less than zero it makes sense for the wavefunction to be negative since all other terms in the integral are positive. This also makes sense since we are adding more degrees of freedom to the system, which means the energy in turn must decrease. In figure 3.4 I have scaled the energy for plotting aesthetics. The actual energy is given by

$$E = -0.626\,\text{MeV}. \tag{3.30}$$

This energy will act as zero-point energy in the rest of the calculations. Note that this energy is found without any considerations about the velocity of the pion below the potential barrier. Strictly speaking, some considerations about the kinematic limit of the pion is needed to more robustly confirm the energy, which is essential to the rest of the calculations.

3.2.2 Relativistic Expansion

It is customary to assume a nonrelativistic limit when considering regular quantum mechanics. To account for relativistic effects we can replace the kinetic term, $K_{\mathbf{r}}$ in (3.18)

$$K_{\mathbf{r}} \rightarrow K_{\mathbf{r},\text{rel}} = \sqrt{p^2c^2 + \mu^2c^4} = \mu c^2\left(\sqrt{1 + \frac{p^2}{\mu^2c^2}} - 1\right), \tag{3.31}$$

where μ is the reduces mass of the nucleon-pion system. This leads to a new systems of equations and these solutions can be compared found in the nonrelativistic limit to deduce with relativistic regime dominates the physical setup. More specifically we can compare the energy ratios denoted by E_R. Starting from (3.20)

$$f(r)(\boldsymbol{\tau}\cdot\boldsymbol{\pi})(\boldsymbol{\sigma}\cdot\mathbf{r})\psi_p + \mu c^2\left(\sqrt{1 + \frac{p^2}{\mu^2c^2}} - 1\right)\psi_{N\pi} = (E - m_\pi c^2)\psi_{N\pi}, \tag{3.32}$$

This equation turns out to be divergent and we must therefor resort to an approximation. The kinetic energy is expanded

$$K_{\mathbf{r},\text{rel}} = \mu c^2\sqrt{1 + \frac{p^2}{\mu^2}} - \mu c^2 \approx \frac{p^2}{2\mu} - \frac{p^4}{8\mu^3c^2} \tag{3.33}$$

This means we get an extra term in (3.23) yielding

$$f(r)\mathbf{r} - \left(\frac{p^2}{2\mu} - \frac{p^4}{8\mu^3c^3}\right)\mathbf{r}\phi(r) = (E - m_\pi c^2)\mathbf{r}\phi(r) \tag{3.34}$$

5. Using the vector operators yields the following expression[5]

$$\begin{aligned}\nabla^4(\mathbf{r}\phi(r)) &= \nabla^2(r\phi'' + 4\phi') \\ &= 2\phi'''' + 2(\nabla\phi''\cdot\nabla)r + 4\phi f'(r) \\ &= r\phi'''' + 6\phi'''\end{aligned} \qquad -\frac{\hbar^2}{2\mu}\left(\phi^{(2)}(r) + \frac{4}{r}\phi^{(1)}(r)\right) + \frac{\hbar^3}{8\mu^3c^3}\left(\phi^{(4)}(r) + \frac{6}{r}\phi^{(3)}(r)\right) = (E - m_\pi c^2)\phi(r), \tag{3.35}$$

where the exponent, (n), is the order the differentiation. This leads to a system of equations given by

$$\left.\begin{aligned} &12\pi\int_0^\infty \mathrm{d}r\, f(r)\phi(r)r^4 = E \\ &f(r) - \tfrac{\hbar^2}{2\mu}\left(\phi^{(2)}(r) + \tfrac{4}{r}\phi^{(1)}(r)\right) + \tfrac{\hbar^4}{8\mu^3c^3}\left(\phi^{(4)}(r) + \tfrac{6}{r}\phi^{(3)}(r)\right) = (E - m_\pi c^2)\phi(r)\end{aligned}\right\} \tag{3.36}$$

This system is a fourth order differential equation coupled to an integrodifferential equation and is solved using the boundary value problem technique. The boundary conditions can be found using the same considerations as in the previous section. For $r \rightarrow \infty$ the dominating terms are

$$\phi^{(4)}(r) = 8\mu^3(E - m_\pi c^2)\phi^{(1)}(r) + 4\mu\phi^{(2)}(r) \tag{3.37}$$

The solutions are shown in figure 3.5

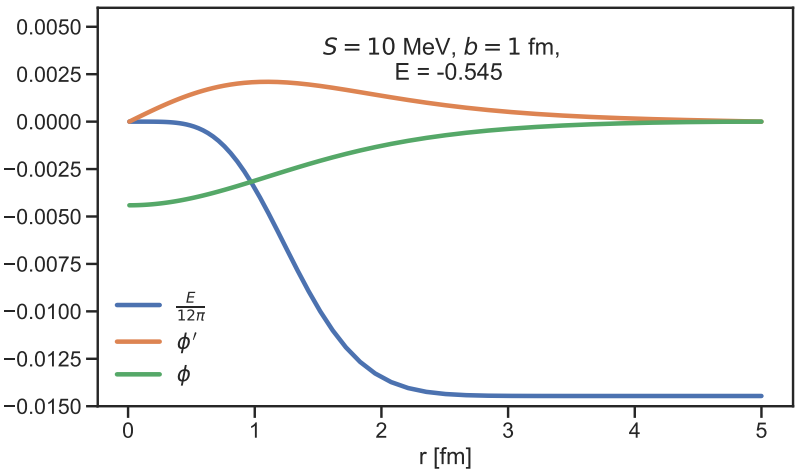

Figure 3.5: Boundary value problem solutions for the relativistic expansion. The plot is generated using a tolerance of 10^{-3}. The energy convergence is scaled.

Since we ultimately want to get values for S and b it is nice to get some intuition behind the behavior of the solutions as we vary these two parameters. This is shown in figure 3.6.

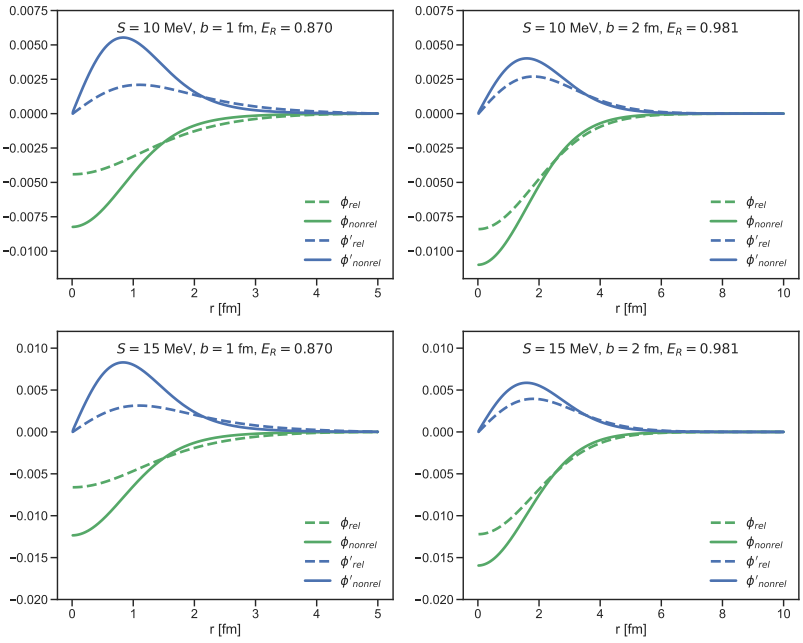

Figure 3.6: Plots for different values of the parameters S and b to illustrate the difference between the nonrelativistic equations and the relativistic equations.

From figure 3.6 one can also deduce the effect of changing the parameters S, b. Increasing the parameter b will flatten the wavefunction which will decrease the energy. This corresponds to increasing the distance between the pion and the nucleus. Increasing the coupling strength S will increase the amplitude of the wave function. In (3.6) we assumed a form but this could might as well be an exponential or even Yukawa-like. We should keep in mind that this form factor greatly impacts the behavior of the system; both in relation to the boundary conditions and the length scale of the wave function.

3.2.3 Different form factors

Compared to conventional interaction models of the nucleus this model has the advantage of having very few parameters. The phenomenological form factor $f(r)$ only consists of an interaction strength S and a range

parameter b. Essentially all the complicated interactions from other nuclear models are hidden in these two parameters and their behavior as a function of the nuclear length, r. We do, however, not know the exact way in which these are related and we must therefore make an educated guess. On figure 3.7 the same problem is solved as in 3.2.1 but the form factor is Yukawa-like, that is

$$f(r) = \frac{S}{b}\frac{\exp\{-1.4r\}}{r} \tag{3.38}$$

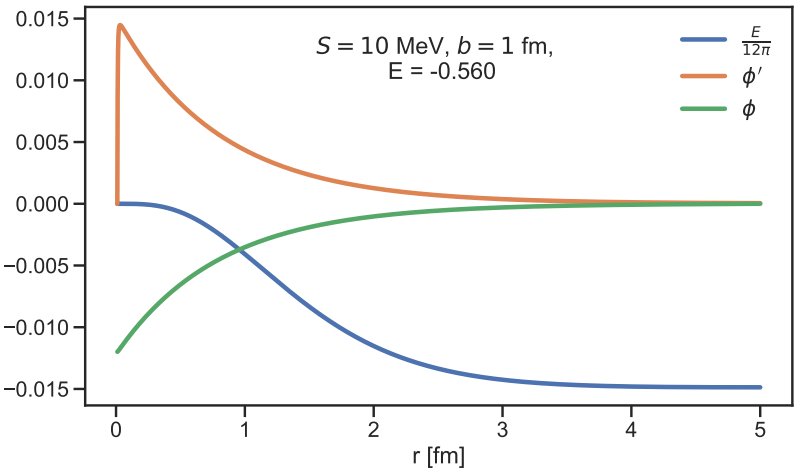

Figure 3.7: Boundary value problem solutions for a Yukawa-like form factor. The plot is generated using a tolerance of 10^{-6}. The RMS values of the relative residuals over each mesh intervals is shown in the Appendix. For clarity, the energy is scaled.

Note the scaling of the exponential is somewhat arbitrary.

Chapter 4

Pion photoproduction

We now consider the case of pion photoproduction. In the model mentioned in section 3.1 the nucleon is in a superposition of states with an arbitrary number of pions. We can write a general multicomponent wavefunction of the nucleon as

$$\Psi_N = \begin{bmatrix} \psi_N \\ \psi_{N\pi} \\ \psi_{N\pi\pi} \\ \vdots \end{bmatrix}, \tag{4.1}$$

where ψ_p is the wave function of the isolated nucleon and $\psi_{N\pi}$ is a system consisting of the nucleon and one pion and the same logic applies to the different wavefunctions. We will refer to the systems with one or more pions as dressed nucleon states in the sense that the isolated nucleon is dressed by a cloud of virtual pions–this is illustrated in figure 4.1. It is important to stress the fact that these are virtual pions. This means in order to generate a pion some energy $m_\pi c^2 \approx 140$ MeV must be added to the system. Within this framework, pion photoproduction comes naturally through photodisintegration. In order words, we disintegrate the nucleon-pion system and create pions in the process. More specifically we disintegrate a two-body system and this is photoproduction within the framework of this model. The disintegration approach is inspired by another two-component system, the deuteron. We, therefore, expect the same approach to apply here. Deuteron photodisintegration is covered in Appendix A. We consider an initial (bound) state given by

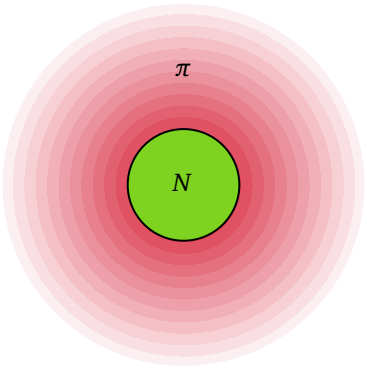

Figure 4.1: Illustration of the dressed nucleon. In the centre (green) is a nucleon and surrounding it is a cloud of virtual pions (red gradient).

$$|\Phi_i\rangle = \begin{bmatrix} \phi_p \\ \phi_{N\pi} \end{bmatrix}, \tag{4.2}$$

where ϕ represents a bound state. The final state consists of the same superposition but in an unbound system represented by ψ, i.e.

$$\left|\Psi_f\right\rangle = \begin{bmatrix} \psi_p \\ \psi_{N\pi} \end{bmatrix}. \tag{4.3}$$

Note that we only consider one-pion systems since we expect this to be largest contribution to the dressed nucleon–nontheless this is an approximation.

4.0.1 Normalization of the initial state

We must also impose some normalization. Starting from (4.2)

$$\Phi = \mathcal{N}\begin{bmatrix} p\uparrow \\ (\boldsymbol{\tau}\cdot\boldsymbol{\pi})(\boldsymbol{\sigma}\cdot\mathbf{r})p\uparrow \phi(r) \end{bmatrix}, \tag{4.4}$$

where $\uparrow$ represents the spin state, $\phi(r)$ is the wavefunction from figure 3.4 and $\mathcal{N}$ is the normalization constant. This leads to

$$\langle\Phi|\Phi\rangle = |\mathcal{N}|^2 \left(\langle\phi_p|\phi_p\rangle + \langle\phi_{N\pi}|\phi_{N\pi}\rangle \right) \tag{4.5}$$

$$= |\mathcal{N}|^2 \left(V + 3V \int \mathrm{d}^3 r\, r^2 \phi(r)^2\right) \tag{4.6}$$

$$\stackrel{!}{=} 1. \tag{4.7}$$

This leads to the following normalization constant

$$\mathcal{N} = \frac{1}{\sqrt{V}} \frac{1}{\sqrt{1+\epsilon}}, \tag{4.8}$$

where V is the volume and ϵ is the integral in (4.6). To figure out what particle can be knocked out by a photon via photodisintegration we consider the pion channel in (4.3). This expression is the properly normalized initial state.

4.0.2 Normalization of the final state

The final state consists of the unbound system represented by ψ. Expanding the terms using the isospin operators yields[1]

$$\phi_{N\pi} = c(\boldsymbol{\tau}\cdot\boldsymbol{\pi})(\boldsymbol{\sigma}\cdot\mathbf{r})p\uparrow\phi(r) = c(p\pi^0 + \sqrt{2}n\pi^+)(\boldsymbol{\sigma}\cdot\mathbf{r})\uparrow\phi(r). \tag{4.9}$$

From this equation, the first result should be highlighted. We consider two photodisintegration processes

$$p\gamma \to p\pi^0 \tag{4.10}$$

$$p\gamma \to n\pi^+, \tag{4.11}$$

where due to orthogonality of the states in isospin space the process involves the neutron is proportional to $\sqrt{2}$. Since this term will exist throughout the calculations we know the ratio between these two processes must be related by a factor of 2. There are also some corrections related to the mass difference between the proton and the neutron. This will be evident when comparing the matrix elements in section 4.0.3.

This expansion will be useful when evaluating matrix elements with the different spin states represented by $(\uparrow\downarrow)$. Considering the final state which consists of a plane wave. It is useful to expand this in terms of spherical harmonics. Using the spherical harmonic decomposition of the plane wave yields

$$\frac{1}{\sqrt{V}}\mathrm{e}^{-i\mathbf{q}\cdot\mathbf{r}} = \frac{1}{\sqrt{V}} \sum_{\ell,m} 4\pi i^\ell Y_\ell^{*m}(\mathbf{q}) Y_\ell^m(\mathbf{r}) j_\ell(qr) \tag{4.12}$$

$$= \frac{1}{\sqrt{V}} \sum_{\ell} 4\pi i^\ell j_\ell(qr) \left(\frac{2\ell+1}{4\pi}\right) P_\ell(\cos\theta), \tag{4.13}$$

where θ is the angle between $\mathbf{q}$ and $\mathbf{r}$ also illustrated on 4.2 and P_ℓ is the Legendre polynomial of degree ℓ. For now $\mathbf{q}$ is some variable related to the energy of the photon and will act as momentum. This is illustrated on figure 4.3 and is expanded upon in the next section. Also, the spherical harmonic addition theorem has been used.[2] Since we are considering the pion channnel just above the threshold we do the following expansion

$$\frac{1}{\sqrt{V}}\mathrm{e}^{i\mathbf{q}\cdot\mathbf{r}} \stackrel{\ell=0}{=} \frac{1}{\sqrt{V}} j_0(qr), \tag{4.14}$$

which is assumed to be the dominant contribution

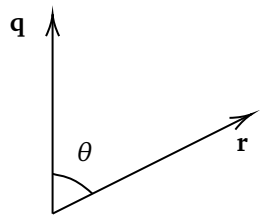

Figure 4.2: Illustration of the angle between the two vectors $\mathbf{q}$ and $\mathbf{r}$ in equation (4.14)

1. $\tau_0\pi^0 + \sqrt{2}\tau_+\pi^- + \sqrt{2}\tau_-\pi^+$

2. $\sum_m Y_\ell^m(\mathbf{p}')Y_\ell^{*m}(\mathbf{r}) = \left(\frac{2\ell+1}{4\pi}\right)P_\ell(\cos\theta)$

4.0.3 Photoproduction: dipole approximation

Having properly normalized the initial and final states we now move on to the actual matrix element we want to calculate. As the normalization of the final state suggests we limit ourselfs to dipole transitions. This is an approximation and contraints the cross section to only be correct for low energies. In order works this should only apply for photon energies just above the threshold. We now want to calculate the matrix element in within the dipole approximation, that is

$$\left\langle \Psi_f \middle| \mathbf{d} \middle| \Phi_i \right\rangle, \tag{4.15}$$

where $\mathbf{d}$ is the dipole operator, $|\Phi_i\rangle$ and $\left|\Psi_f\right\rangle$ are given by (4.2) and (4.3) respectively. As before, we only consider the pion channel. Since we are considering transitions just above the threshold we only consider the contributions from the electric dipole term. This terms is assumed to dominate and higher order terms can be calculated later if necessary. Considering the pion channel for the following process $p\gamma \to n\pi^+$

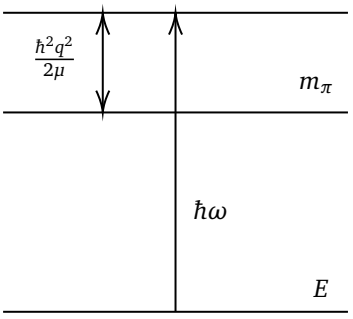

Figure 4.3: Illustration of the energy levels. Here the energy E refers to the energy shown in 3.4 and will act as a zero-point energy.

$$\mathcal{M} = -i\omega_k \sqrt{\frac{2\pi\hbar}{V\omega_{\mathbf{k}}}} \mathbf{e}_{\mathbf{k},\lambda} \left\langle \frac{1}{\sqrt{V}} e^{i\mathbf{q}\cdot\mathbf{r}} n\pi^+(\uparrow\downarrow) |\mathbf{d}| (\boldsymbol{\tau}\cdot\boldsymbol{\pi})(\boldsymbol{\sigma}\cdot\mathbf{r}) p\uparrow \phi(r)\mathcal{N} \right\rangle \tag{4.16}$$

where the two arrows represent the two spin states of the neutron and the proton. Also, q is illustrated in figure 4.3 where the energy, E, is the same as in (3.25). This is the zero point energy in the system we are considering and can be written as

$$\frac{\hbar^2 q^2}{2\mu_{N\pi}} = \hbar\omega - m_\pi c^2, \tag{4.17}$$

where $\mu_{N\pi}$ is the reduced mass of the nucleon-pion system. Compare this equation to (A.22). The front factor arises from the quantization of the electromagnetic field. Using the results from section 4.0.2 and section 4.0.1. The different spin states of the neutron in the final state yields to contributions to the total matrix element given by

$$\mathcal{M}^\uparrow = \frac{-i\mathcal{N}\sqrt{2}\omega_k \mathbf{e}_{\mathbf{k},\lambda}}{V} \sqrt{\frac{2\pi\hbar}{V\omega_{\mathbf{k}}}} \langle j_0(qr)|d_0 r_0|\phi(r)\rangle \tag{4.18}$$

$$= \frac{-i\mathcal{N}\sqrt{2}\omega_k \mathbf{e}_{\mathbf{k},\lambda}}{V} \sqrt{\frac{2\pi\hbar}{V\omega_{\mathbf{k}}}} \sqrt{\frac{4\pi}{3}} \langle j_0(qr)|d_0 r Y_1^0|\phi(r)\rangle \tag{4.19}$$

$$\mathcal{M}^\downarrow = \frac{-i\mathcal{N}2\omega_k \mathbf{e}_{\mathbf{k},\lambda}}{V} \sqrt{\frac{2\pi\hbar}{V\omega_{\mathbf{k}}}} \left\langle j_0(qr)\middle|dr_+\middle|\phi(r)\right\rangle \tag{4.20}$$

$$= \frac{-i\mathcal{N}2\omega_k \mathbf{e}_{\mathbf{k},\lambda}}{V} \sqrt{\frac{2\pi\hbar}{V\omega_{\mathbf{k}}}} \sqrt{\frac{4\pi}{3}} \langle j_0(qr)|d_0 r Y_1^1|\phi(r)\rangle, \tag{4.21}$$

$$\tag{4.22}$$

where the spin down state picks up a factor $\sqrt{2}$ from equation 3.5. Now

we calculate the remaining matrix elements,

$$\left\langle j_0(qr)\middle|d_0 r_0\middle|\phi(r)\right\rangle = \frac{\mu}{m_\pi} e \left\langle j_0(qr)\middle|r_0 r_0\middle|\phi(r)\right\rangle \tag{4.23}$$

$$= \frac{\mu}{m_\pi} e \frac{4\pi}{3} \left\langle j_0\middle|r^2\middle|\phi(r)\right\rangle \tag{4.24}$$

$$= \frac{\mu e}{m_\pi} \int_0^\pi \int_0^{2\pi} \int_0^\infty \mathrm{d}r\mathrm{d}\phi\mathrm{d}\theta\, j_0(qr) r^4 \cos^2\theta \sin\theta \phi(r) \tag{4.25}$$

$$= \frac{4\pi\mu e}{3m_\pi} \underbrace{\int_0^\infty \mathrm{d}r\, j_0(qr) r^4 \phi(r)}_{Q(r)}, \tag{4.26}$$

where the dipole operator has been inserted and the angular integrals calculated. Similarly for the next matrix element,

$$\left\langle j_0(qr)\middle|d_- r_+\middle|\phi(r)\right\rangle = \frac{\mu}{m_\pi} e \left\langle j_0(qr)\middle|r_- r_+\middle|\phi(r)\right\rangle \tag{4.27}$$

$$= \frac{4\pi\mu e}{3m_\pi} \left\langle j_0(qr)\middle|r^2 Y_1^{-1} Y_1^1\middle|\phi(r)\right\rangle \tag{4.28}$$

$$= \frac{4\pi\mu e}{3m_\pi} Q. \tag{4.29}$$

This leads to the two final expressions for the two matrix elements

$$\left|\mathcal{M}^\uparrow\right| = \left(\frac{4\pi\mu e}{3m_\pi}\right)^2 \frac{2\mathcal{N}^2\omega_k(2\pi\hbar)}{V^2} (\mathbf{e}_{\mathbf{k},\lambda})^0 (\mathbf{e}^*_{\mathbf{k},\lambda})^0 Q^2 \tag{4.30}$$

Similarly for the next matrix element

$$\left|\mathcal{M}^\downarrow\right| = \left(\frac{4\pi\mu e}{3m_\pi}\right)^2 \frac{4\mathcal{N}\omega_{\mathbf{k}}(2\pi\hbar)}{V^2} (\mathbf{e}_{\mathbf{k},\lambda})^+ (\mathbf{e}^*_{\mathbf{k},\lambda})^+ Q^2. \tag{4.31}$$

3. $(\mathbf{e}^*_{\mathbf{k},\lambda} \cdot \mathbf{e}_{\mathbf{k},\lambda}) = \delta_{\lambda,\lambda'}$ and $\mathbf{e}_{\mathbf{k},\mp} = \pm\frac{1}{\sqrt{2}}(\mathbf{e}_{\mathbf{k},1} \pm i\mathbf{e}_{\mathbf{k},2})$. This leads to $(\mathbf{e}^{0*}_{\mathbf{k},\lambda} \cdot \mathbf{e}^0_{\mathbf{k},\lambda'}) + (\mathbf{e}^{0+}_{\mathbf{k},\lambda} \cdot \mathbf{e}^+_{\mathbf{k},\lambda'}) = \delta_{\lambda,\lambda'} + \frac{1}{2}\delta_{\lambda,\lambda'}$

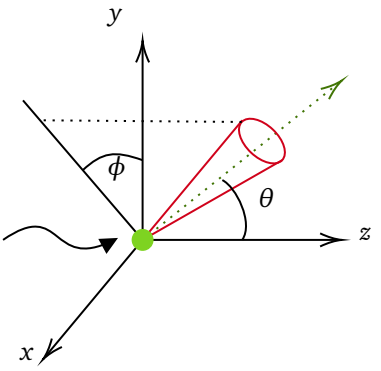

Figure 4.4: Illustration of the differential cross section.

Calculating the total matrix element using a polarization theorem[3]

$$|\mathcal{M}|^2 = \left|\mathcal{M}^\uparrow\right|^2 + \left|\mathcal{M}^\downarrow\right|^2 \tag{4.32}$$

$$= \frac{2\pi\hbar\omega_k \mathcal{N}^2 e^2}{V^2} \left(\frac{4\pi\mu}{3m_\pi}\right)^2 Q^2, \tag{4.33}$$

which is the final expression for the matrix element. According to Fermi's golden rule we can calculate the transition probability

$$\mathrm{d}\omega = \frac{2\pi}{\hbar} |\mathcal{M}|^2 \,\mathrm{d}\rho, \tag{4.34}$$

where the density of states is given by

$$\mathrm{d}\rho = \frac{Vqm}{\hbar^2(2\pi)^3} \mathrm{d}\Omega. \tag{4.35}$$

This is related to the differential cross section

$$\frac{\mathrm{d}\sigma}{\mathrm{d}\Omega_q} = \frac{16\pi}{9} \mathcal{N}^2 \alpha \frac{kq\mu_{N\pi}^3}{m_\pi^2 \hbar c} Q^2, \tag{4.36}$$

and since there is no explicit angular dependency the total cross section is given by

$$\sigma_{\text{dipole}} = \oint_{4\pi} \frac{\mathrm{d}\sigma}{\mathrm{d}\Omega_q} \mathrm{d}\Omega_q \tag{4.37}$$

$$= 4\pi \frac{16\pi}{9} \mathcal{N}^2 \alpha \frac{kq\mu_{N\pi}^3}{m_\pi^2 \hbar c} Q^2 \tag{4.38}$$

$$= \frac{64\pi^2}{9} \mathcal{N}^2 \alpha \frac{kq\mu_{p\pi}^3}{m_\pi^2 \hbar c} \left(\int_0^\infty \mathrm{d}r \, j_0(qr) r^4 \phi(r) \right)^2 . \tag{4.39}$$

This is the final expression for the total cross section of protoproduction of charged pions using the dipole approximation. We now perform a fit to experimental data for the parameters S and b and enter in the wave function $\phi(r)$. Here two considerations are needed. Both the dipole approximation and the one-pion approximation limit the validity of the cross section to near threshold. And due to the limited amount of experimental data for charged pion photoproduction the fit is limited to approximately 15 MeV from the threshold. This means some data points are excluded to constrain the fitted parameters to values that might seems physically realistic.

The fit is performed and can be seen on figure 4.5.

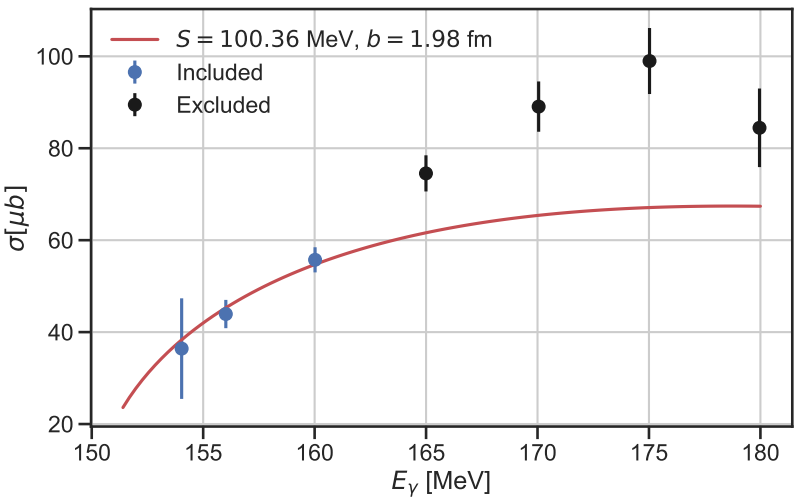

Figure 4.5: The total cross section of the photoproduction process $\gamma p \to \pi^+ n$ fitted to experimental data. The fit parameters are shown in the figure. The blue data points are included in the fit and the black data points are excluded since these violate both the dipole and the one pion approximation.

The parameters S and b seem reasonable but more importantly we are interested in the relative weight coming from the $N\pi$ component in the wave function and the virtual pions contribution to the dressed proton. This corresponds to solving the equations in (3.25) with the new parameters. The contribution to the wave function is calculated as follows

$$\int_V \mathrm{d}^3R \int_V \mathrm{d}^3r \left|\psi_{N\pi}\right| = 4\pi \int_0^\infty \mathrm{d}r \, \phi(r)^2 r^2 \tag{4.40}$$

$$= 0.69 \tag{4.41}$$

using (3.13) and considering only the π^+ component in $\boldsymbol{\pi}$. The energy is calculated which yields

$$E_{\text{virtual pions}} = -449\,\text{MeV}. \tag{4.42}$$

Note here that we have used two approximations that limit (4.39) to energies very close to the treshold. To futher test the validity of the

model we need a more general expression for the cross section and more data points. This means we have to consider the exact matrix element for the transition and consider the photoproduction of neutral pions off protons since this is the most experimentally investigated photoproduction process.

4.1 Pion Photoproduction exact

In section 4 we looked at how to use the model described in section 3.1 to get an expression for the cross-section which was compared to experimental data. More specifically we used the dipole approximation which introduces a trade-off between the difficulty of the calculations and the regime in which our solution is valid. We expect the dipole approximation to hold for low energies just above the threshold. To both validate and generalize this result we now do a different approach and calculate the cross-section exact and also consider recoil effects. Strictly speaking, recoil effects should also be considered in section 4 since the mass ratio between the nucleon and the pion cannot be assumed to yield a stationary nucleon after the pion photoproduction process. To calculate the exact matrix elements we consider a non-relativistic system of particles interacting with the electromagnetic field. The interacting part of the Hamiltonian is given by

$$H = \frac{1}{2m_\pi}\left(\mathbf{p} - \frac{e}{c}\mathbf{A}(\mathbf{r})\right)^2, \tag{4.43}$$

where $\mathbf{p}$ is the momentum operator and $\mathbf{A}(\mathbf{r})$ is the quantized vector potential at the point $\mathbf{r}$. Note that we have already replaced the usual mass by the mass of the pion, m_π since we are considering the interaction of a pion with charge e with the electromagnetic field.

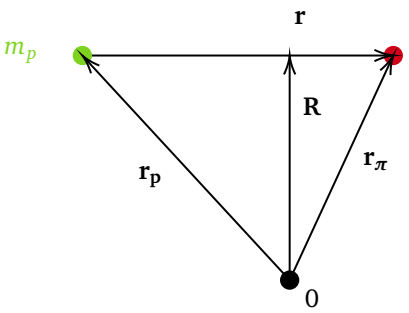

Figure 4.6: Jacobi coordinates illustrating $\mathbf{r}_\pi$ used in the vector potential in equation 4.46. Here we use $\mathbf{r} = \mathbf{r}_\pi - \mathbf{r}_p$ and see that $\mathbf{r}_\pi = \mathbf{R} + \mathbf{r}\frac{m_p}{M_{p\pi}}$, where $M_{p\pi} = m_p + m_\pi$.

The electromagnetic interaction is relatively weak compared to the strong force. For our problem, this means we can expand the interaction by taking only the lowest non-vanishing order of perturbation into account. Since we later want to consider transition probabilities we only keep the first non-linear term of (4.43) which yields

$$V^{(1)} = -\frac{e}{2m_p c}\Big(\mathbf{p}\cdot\mathbf{A}(\mathbf{r}_p,t) + \mathbf{A}(\mathbf{r}_p,t)\cdot\mathbf{p}\Big), \tag{4.44}$$

which also means the interacting part is linear in the creation(annihilation) operators corresponding to single-photon emission(absorption). Our choice of gauge is purely conventional and we choose the radiation gauge which imposes a condition on the vector potential given by

$$\nabla\cdot\mathbf{A} = 0, \tag{4.45}$$

and this is a convenient choice of gauge since the commutator in (4.44) is $\nabla\cdot\mathbf{A}$ and we can write

$$V^{(1)} = -\frac{e}{m_p c}\mathbf{A}(\mathbf{r_p},t)\cdot\mathbf{p}_p. \tag{4.46}$$

Note that (4.46) consists of the pion momentum operator, $\mathbf{p}_\pi$ and the electromagnetic vector potential at a distance r_π. This distance was also mentioned in section 3.1 and can be expressed in term of the Jacobi coordinates illustrated on figure 4.6 where the relative coordinate is given by $\mathbf{r} = \mathbf{r}_\pi - \mathbf{r}_p$ which leads to the following transformation of equation (4.46)

$$V^{(1)} = -\frac{e}{m_p c}\mathbf{A}(\mathbf{r_p},t)\cdot\mathbf{p}_p = -\frac{e}{m_p c}\mathbf{A}\left(\mathbf{R} - \frac{m_\pi}{M_{p\pi}}\mathbf{r},t\right)\left(\frac{m_p}{M_{p\pi}}\mathbf{P} - \mathbf{p}\right), \tag{4.47}$$

where $M_{p\pi} = m_p + m_\pi$ is the total mass of the system and $\mathbf{R}$ is the coordinate vector for the center of mass. We now move on from the general theory of the pion interacting with the electromagnetic field and consider the specific case of pion photoproduction. To recap we consider the following processes

$$p\gamma \to p\pi^0 \tag{4.48}$$
$$p\gamma \to n\pi^+ \tag{4.49}$$
$$n\gamma \to n\pi^0 \tag{4.50}$$
$$n\gamma \to p\pi^-, \tag{4.51}$$

where the initial states consist of a dressed proton or neutron and a plane wave photon which in the language of 2nd quantization can be written as $a^\dagger_{\mathbf{k},\lambda}|0\rangle$ corresponding to creating a photon with wave vector $\mathbf{k}$ and polarization λ from the vacuum $|0\rangle$. The final states consists of a nucleon and a pion and no photon, i.e electromagnetic vacuum. This leads to the following expression for the matrix element for the transitions in (4.48), (4.49), (4.50) and (4.51)

$$\frac{-e}{m_\pi c}\langle 0|\mathbf{A}\big(\mathbf{R} - \frac{m_\pi}{M_{p\pi}}\mathbf{r}, t\big)a^\dagger_{\mathbf{k},\lambda}|0\rangle = \frac{-e}{m_p}\sqrt{\frac{2\pi\hbar}{\omega_\mathbf{k} V}}\mathbf{e}_{\mathbf{k},\lambda}e^{i\mathbf{k}(\mathbf{R}-\frac{m_\pi}{M_{p\pi}}\mathbf{r})-i\omega_k t}. \tag{4.52}$$

Completely analogous to section 4.0.3 and specifically equation (4.34) we now want to consider the probability of transition per unit time of going from the initial state $|i\rangle$ to $\langle f|$ according to Fermi's golden rule

$$\mathrm{d}\omega = \frac{2\pi}{\hbar}|\mathcal{M}|^2\,\mathrm{d}\rho, \tag{4.53}$$

where $\mathrm{d}\rho$ is the density of states also analogous to (4.35). The difference is that we do not employ the dipole approximation to evaluate the matrix element $\mathcal{M}$ and we also consider recoil. In the following section we focus on pion photoproduction of neutral pion off protons corresponding to the transition in (4.48). The choice is due to the fact that there is a lot more experimental data available for pion photoproduction off protons compared to neutrons since it is easier to achive experimentally. We focus on neutral pions since our one-pion approximation is assumed to be valid near the threshold and since we are interested in fitting to experimental data we need as much data near the threshold as possible–and this is the case for neutral pion photoproduction

4.1.1 Neutral Pion Phototoproduction off Protons

From (4.52) we get

$$\mathcal{M}^{(\uparrow\downarrow)} = \frac{e}{m_p}\sqrt{\frac{2\pi\hbar}{\omega_\mathbf{k}V}}\langle(\uparrow\downarrow)p\pi^0|\frac{e^{i\mathbf{q}\cdot\mathbf{r}}}{\sqrt{V}}\frac{e^{i\mathbf{Q}\cdot\mathbf{r}}}{\sqrt{V}}|e^{i\mathbf{k}(R-\frac{m_\pi}{M_{p\pi}}\mathbf{r})}(\mathbf{e}_{\mathbf{k},\lambda}\mathbf{p})|(\boldsymbol{\tau}\cdot\boldsymbol{\pi})(\boldsymbol{\sigma}\cdot\mathbf{r})\phi(r)\frac{p\uparrow}{\sqrt{V}}\rangle \tag{4.54}$$
$$= \frac{-e}{m_p}\sqrt{\frac{2\pi\hbar}{\omega_\mathbf{k}V}}\langle(\uparrow\downarrow)\frac{e^{i\mathbf{q}\cdot\mathbf{r}}}{\sqrt{V}}\frac{e^{i\mathbf{Q}\cdot\mathbf{r}}}{\sqrt{V}}|e^{i\mathbf{k}(R-\frac{m_\pi}{M_{p\pi}}\mathbf{r})}(\mathbf{e}_{\mathbf{k},\lambda}\mathbf{p})|(\boldsymbol{\sigma}\cdot\mathbf{r})\phi(r)\frac{\uparrow}{\sqrt{V}}\rangle, \tag{4.55}$$

where we have used $\int \mathrm{d}^3 r e^{i\mathbf{k}\cdot\mathbf{R}} = V$ and $\langle p\pi^0|\boldsymbol{\tau}\cdot\boldsymbol{\pi}|p\rangle = 1$. Note that $\mathbf{q}$ is the wave-number of the pion-proton relative momentum and $\mathbf{Q}$ is originates from conservation of momentum, that is $\mathbf{Q} = \mathbf{k}$. Defining a

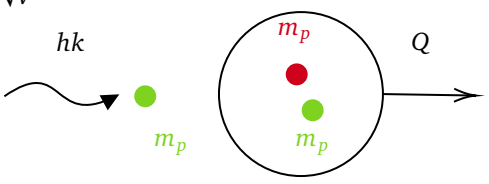

Figure 4.7: Neutral pion photoproduction with conservation of momentum $\mathbf{k} = \mathbf{Q}$ illustrated

new vector, $\mathbf{s} = \mathbf{q} + \frac{m_\pi}{M_{p\pi}}\mathbf{k}$ yields

$$\mathcal{M}^{(\uparrow\downarrow)} = \frac{-e}{m_\pi}\sqrt{\frac{2\pi\hbar}{\omega_\mathbf{k}}}\frac{1}{V}\langle(\uparrow\downarrow)|\langle e^{i\mathbf{s}\cdot\mathbf{r}}|(\mathbf{e}_{\mathbf{k},\lambda}\mathbf{p})(\boldsymbol{\sigma}\cdot\mathbf{r})|\phi(r)\rangle|\uparrow\rangle \tag{4.56}$$

Note the different inner products. We now do the plane wave expansion using (4.12) and consider the angular averaging of two coordinates variables[4]

4. $\int \mathrm{d}\Omega\, n_k n_l = \frac{4\pi}{3}\delta_{kl}$, which means $\int \mathrm{d}\Omega\, r_k r_l = \frac{4\pi r^2}{3}\delta_{kl}$, where n is a unit vector

$$\langle e^{i\mathbf{s}\cdot\mathbf{r}}|(\mathbf{e}_{\mathbf{k},\lambda}\frac{\partial}{\partial\mathbf{r}})(\boldsymbol{\sigma}\cdot\mathbf{r})|\phi(r)\rangle = +i(\mathbf{e}_{\mathbf{k},\lambda}\cdot\mathbf{s})\int \mathrm{d}^3r\, e^{i\mathbf{s}\cdot\mathbf{r}}(\boldsymbol{\sigma}\cdot\mathbf{r})\phi(r) \tag{4.57}$$

$$= -i(\mathbf{e}_{\mathbf{k},\lambda}\cdot\mathbf{s})\int \mathrm{d}^3r\, 3ir j_1(sr)\frac{\mathbf{s}\cdot\mathbf{r}}{sr}(\boldsymbol{\sigma}\cdot\mathbf{r})\phi(r) \tag{4.58}$$

$$= (\mathbf{e}_{\mathbf{k},\lambda}\cdot\mathbf{s})(\boldsymbol{\sigma}\cdot\mathbf{r})\underbrace{\frac{4\pi}{s}\int_0^\infty \mathrm{d}r\, r^3 j_1(sr)\phi(r)}_{F(s)} \tag{4.59}$$

$$= (\mathbf{e}_{\mathbf{k},\lambda}\cdot\mathbf{s})(\boldsymbol{\sigma}\cdot\mathbf{r})F(s). \tag{4.60}$$

Returning to the matrix element (4.55)

$$\mathcal{M}^{(\uparrow\downarrow)} = \frac{ie\hbar}{m_p}\sqrt{\frac{2\pi\hbar}{\omega_k}}\frac{1}{V}\langle(\uparrow\downarrow)|(\mathbf{e}_{\mathbf{k},\lambda}\cdot\mathbf{s})F(s)|\uparrow\rangle \tag{4.61}$$

$$= \frac{ie\hbar}{m_p}\sqrt{\frac{2\pi\hbar}{\omega_k}}\frac{1}{V}(\mathbf{e}_{\mathbf{k},\lambda}\cdot\mathbf{s})\langle(\uparrow\downarrow)|(\boldsymbol{\sigma}\cdot\mathbf{r})|\uparrow\rangle F(s), \tag{4.62}$$

5. We do this step already to use a completeness relation for the polarization.

which leads to the following expression for the norm square[5]

$$\left|\mathcal{M}^{(\uparrow\downarrow)}\right|^2 = \frac{2\pi\hbar^3e^2}{m_p^2\omega_k V^2}\left|\mathbf{e}_{\mathbf{k},\lambda}\cdot\mathbf{s}\right|^2\left|\langle(\uparrow\downarrow)|(\boldsymbol{\sigma}\cdot\mathbf{r})|\uparrow\rangle\right|^2 F(s)^2, \tag{4.63}$$

and now calculating

$$\sum_\lambda = \left|(\mathbf{e}_{\mathbf{k},\lambda}\cdot\mathbf{s})\right|^2 = \sum_\lambda(\mathbf{e}^*_{\mathbf{k},\lambda}\cdot\mathbf{s})(\mathbf{e}_{\mathbf{k},\lambda}\cdot\mathbf{s}) \tag{4.64}$$

$$= s^2 - \frac{(\mathbf{k}\cdot\mathbf{s})^2}{k^2} \tag{4.65}$$

$$= q^2 - \frac{(\mathbf{k}\cdot\mathbf{q})^2}{k^2} \tag{4.66}$$

$$= q^2\sin^2(\theta_q), \tag{4.67}$$

where θ_q is the angle between $\mathbf{k}$ and $\mathbf{q}$ and we now have an angular dependency originating from the dot product. I have added a subscript q to empathize that this relative to the final state momentum $\mathbf{q}$ located in (θ,ϕ) also illustrated on figure 4.4.

Plugging (4.64) into (4.63) yields

$$\frac{1}{2}\sum_{\lambda,(\uparrow\downarrow)}\left|\mathcal{M}_{fi}\right|^2 = \frac{\pi e^2\hbar^3}{V^2m_p^2}\frac{1}{\omega_k}q^2\sin^2(\theta)s^2F(s)^2. \tag{4.68}$$

According to Fermi's golden rule the transition probability is given by

$$\mathrm{d}\omega = \frac{2\pi}{\hbar}|\mathcal{M}|^2\,\mathrm{d}\rho, \quad \mathrm{d}\rho = \frac{V\mu_{p\pi}q}{\hbar^2(2\pi)^3}\mathrm{d}\Omega_q, \tag{4.69}$$

where the density of states in the final state assumes a non-relativistic expansion. Strictly speaking this is an approximation. Also, **q** denotes the differential angle element to empathize that this is relative to the pion-proton system. Plugging (4.68) into (4.69)

$$\mathrm{d}\omega = \frac{e^2}{8\pi}\frac{\mu_{p\pi}c^2}{m_p^2c^4\omega_k}q^3\sin^2(\theta_q)s^2F(s)^2\mathrm{d}\Omega_q \tag{4.70}$$

which leads to the following expression for the differential cross section by considering the time it takes the photon to cross the volume, V.

$$\frac{\mathrm{d}\sigma}{\mathrm{d}\Omega_q} = \frac{e^2}{8\pi}\frac{M_{p\pi}c^2}{m_p^2c^4}\frac{q^3}{k}\sin^2(\theta_q)s^2F(s)^2 \tag{4.71}$$

In (4.71) we have an expression for the angular dependency. This means for some photon energy we get an angular distribution. This can also be compared to experimental data. (This can be done for all the figures in [Beck et al. 1990] and also for charged pions). Figure 4.8 shows the differential cross section as a function of the angle θ_{cm} compared to experimental data.

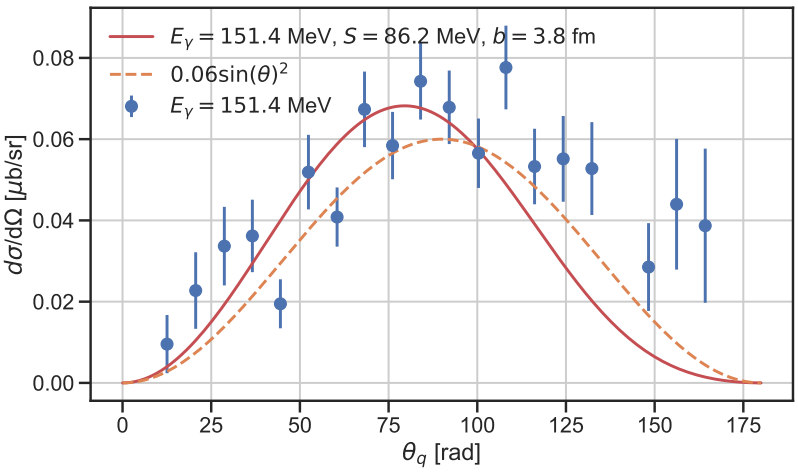

Figure 4.8: Not fitted parameters! Note the dependency is not $\sin(\theta_q)^2$ since there is a contribution from $F(s)$ as well.

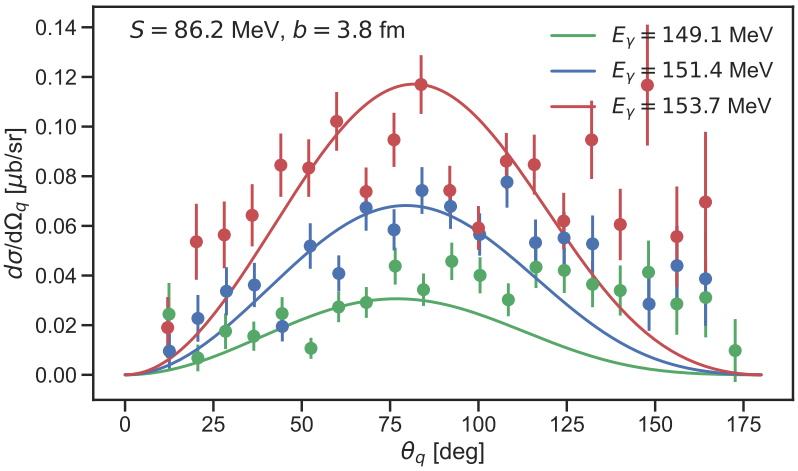

Figure 4.9: Multiple energies

To get an expression for the total cross section equation the expression

is integrated into containing only a radial part using

$$\sigma = 2\pi \int_0^\pi \mathrm{d}\theta \, \sin(\theta_q) \frac{\mathrm{d}\sigma}{\mathrm{d}\Omega_q} \tag{4.72}$$

$$= 2\pi \int_0^\pi \mathrm{d}\theta \, \frac{e^2}{8\pi} \frac{\mu_{p\pi} c^2}{m_p^2 c^4} \frac{q^3}{k} \sin^3(\theta) s^2 F(s)^2 \tag{4.73}$$

(4.72) is fitted to experimental data such that the physical parameters in our model S and b can be extracted. So far the values of these parameters have been chosen at random. However, we do have some intuition about how these two affect the wavefunction of the system from figure 3.6. From (4.72) we see that the wave function only enters explicitly in the integral so the general behavior of the cross section is hard to predict. The fit is done and can be seen in figure 4.10. Data is from [Schmidt et al. 2001]

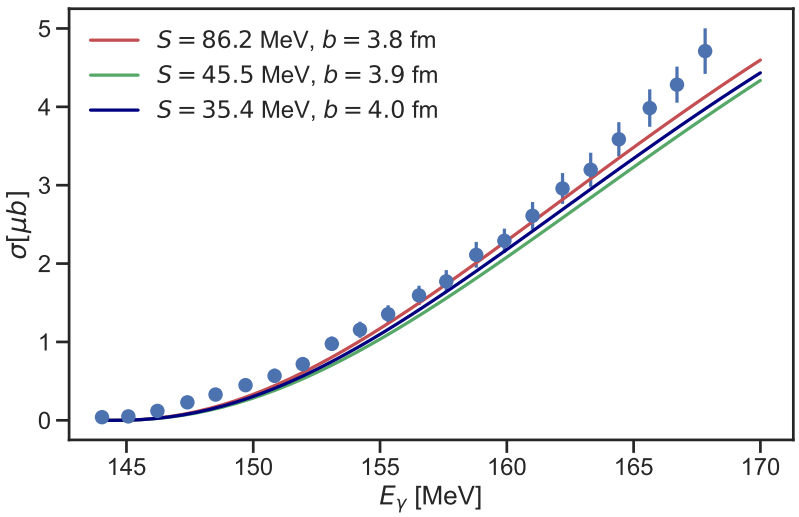

Figure 4.10: Fitted parameters to experimental data for the process $\gamma p \to \pi^0 p$. The fit parameters for S, b are shown inside the figure.

Note that these expressions are for the production of neutral pions. The same approach can be done for charged pions.

There is some freedom of choice in the fit. The integral is slowly converging and a cut-off must be introduced. This cut-off is arbitrary and does affect the fit. For a larger cut-off the line flattens out before 165 MeV. This leads to a more phenomenological discussion of the model in relation to the cross section as a function of energy. For higher energies we expect more than one pion to contribute to the cross section. This model, however, only takes one pion into account. To describe the behavior at higher energies more pions must be taking into account. This highlights the strengths and weaknesses of using differential equations to describe the physical system. If we take more pions into account this approach is no longer favorable since this leads to too many coupled systems. For more pions one would have to resort to another method.

For neutral pion off neutrons

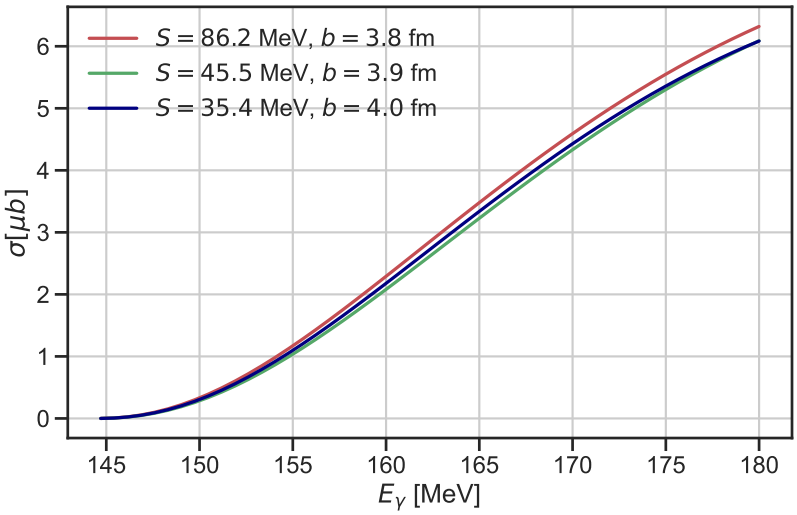

Figure 4.11: The process $\gamma n \to \pi^0 n$ with the same parameters as for neutral pion photoproduction off protons.

4.2 Nuclear Effective Field Theory operator

The construction of the most general chiral Lagrangian is based on the theory of the non-linear realization of a symmetry. The baryon-number-conserving chiral Lagrangian can be split into pieces with even numbers of fermion fields where in this section we will focus on

$$\mathcal{L} = N^\dagger \left(i\mathcal{D}_0 + \frac{\mathcal{D}^2}{2m_N} \right) N + \frac{g_A}{2f_\pi} N^\dagger \boldsymbol{\tau} N \cdot \mathbf{D}\boldsymbol{\pi}, \tag{4.74}$$

where the second term is very similar to the creation operator W from equation (3.16)–only the $\mathbf{r}$ is replaced by $\nabla_\mathbf{r}$. The general operator is constructed in such a way that parity, isospin and spin is conserved and there is some freedom in the choice of the distance operator. In this section we explore the differences, if any, by constructing the nuclear model with explicit mesons with the operator as is it defined in chiral effective field theory. We assume the following form of the wave function of the proton and the system consisting of a nucleon and a single pion

$$\psi_p = p \uparrow \frac{1}{\sqrt{V}}, \quad \psi_{N\pi} = (\boldsymbol{\tau} \cdot \boldsymbol{\pi})(\boldsymbol{\sigma} \cdot \frac{\partial}{\partial \mathbf{r}}) p \uparrow \frac{1}{\sqrt{V}} \phi, \tag{4.75}$$

where $\boldsymbol{\tau}$ and $\boldsymbol{\sigma}$ are vectors consistsing of Pauli matrices acting on isospin and spin space on the nucleon respectively. $\boldsymbol{\pi}$ is the isovector of pions. We now construct an operator to create and annihilate a pion

$$W = (\boldsymbol{\tau} \cdot \boldsymbol{\pi})(\boldsymbol{\sigma} \cdot \frac{\partial}{\partial \mathbf{r}}) f(r) \tag{4.76}$$

$$W^\dagger = \int_V \mathrm{d}^3 r \, (\boldsymbol{\tau} \cdot \boldsymbol{\pi})^\dagger (\boldsymbol{\sigma} \cdot \frac{\partial}{\partial \mathbf{r}})^\dagger f(r), \tag{4.77}$$

where $f(r)$ is a form factor. The annihilation operator must contain the integral to remove the coordinate of the pion. This leads to the following Schrödinger equation

$$\begin{bmatrix} K_\mathbf{R} & W^\dagger \\ W & K_\mathbf{R} + K_\mathbf{r} + m_\pi c^2 \end{bmatrix} \begin{bmatrix} \psi_p \\ \psi_{N\pi} \end{bmatrix} = E \begin{bmatrix} \psi_p \\ \psi_{N\pi} \end{bmatrix}, \tag{4.78}$$

which is expanded

$$12\pi \int_0^\infty \mathrm{d}r \, \frac{\partial^2}{\partial r^2} r^2 f(r)\phi(r) = E \tag{4.79}$$

$$\frac{\partial}{\partial r} f(r) - \frac{2\hbar^2}{\mu_{N\pi}} \frac{\partial^3}{\partial r^3} \phi(r) = (E - m_\pi c^2) \frac{\partial}{\partial r} \phi(r). \tag{4.80}$$

Assume the form factor is on the following form

$$f(r) = \frac{S}{b} \mathrm{e}^{-r^2/b^2} \tag{4.81}$$

which yields

$$\frac{\partial}{\partial r} f(r) = \frac{-2r}{b^2} f(r), \quad \frac{\partial^2}{\partial r^2} = -\frac{2(b^2 - 2r^2 2)}{b^4} f(r). \tag{4.82}$$

The terms inside the integral in equation (4.79)

$$\frac{\partial^2}{\partial r^2}(r^2 f(r)\phi(r)) = 2rf(r)\phi(r) + 2rf'(r)\phi(r) + r^2 f(r)\phi'(r) \tag{4.83}$$

$$+ 2rf'(r)\phi(r) + r^2 f''^{(r)}\phi(r) + r^2 f'(r)\phi'(r) \tag{4.84}$$

$$+ 2rf(r)\phi(r) + r^2 f'(r)\phi'(r) + r^2 f(r)\phi''(r) \tag{4.85}$$

$$\equiv Y(r) \tag{4.86}$$

Considering the limits of (4.80) which for large r is

$$-\frac{2\hbar^2}{\mu_{N\pi}} \phi'''(r) = (E - m_\pi c^2)\phi'(r) \tag{4.87}$$

The solution is shown on 4.12

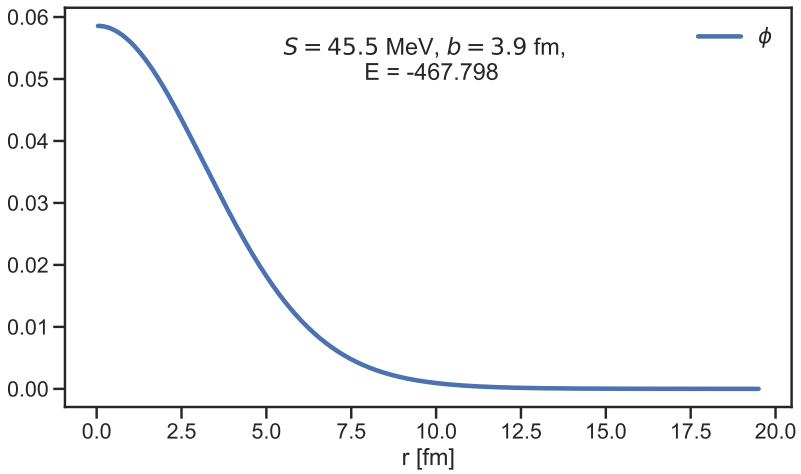

Figure 4.12: Fitted parameters to experimental data. The fit parameters for S, b are shown inside the figure.

Appendix A

Nuclear photoeffect and the deuteron

In this appendix, I wish to go through how to get expressions for the differential cross section and the total cross section from the wave function. The wave function can be obtained analytically or numerically – in this appendix, I will sketch an analytical approach to s-wave calculations. Considering the central potential between the proton and the neutron given by

$$U(r) = \begin{cases} -U_0, & r \leq R \\ 0 & r > R \end{cases}$$

The radial equation is given by

$$-\frac{\hbar^2}{2m}\frac{\mathrm{d}^2u(r)}{\mathrm{d}r^2} + \left[U(r) + \frac{\hbar^2\ell(\ell+1)}{2mr^2}\right]u(r) = Eu(r). \tag{A.1}$$

This is identical to the one-dimensional Schrodinger equation with an effective potential, where the centrifugal term pushes the particle outwards. To solve this analytically I rewrite the equation and consider the boundary conditions.

$$\frac{\mathrm{d}^2u(r)}{\mathrm{d}r^2} + \frac{M}{\hbar^2}\left[E - U(r)\right]u(r) = 0, \tag{A.2}$$

where I plugged in the expression for the reduced mass, $m = M/2$. For the deuteron I use $E = -E_B = -2.225$ MeV [Zelevinsky and Volya 2017, p. 51]. This leads to the following expressions

$$\frac{\mathrm{d}^2u(r)}{\mathrm{d}r^2} + \frac{M}{\hbar^2}\left(U_0 - E_B\right)u(r) = 0, \quad r \leq R, \tag{A.3}$$

$$\frac{\mathrm{d}^2u(r)}{\mathrm{d}r^2} - \frac{M}{\hbar^2}E_B u(r) = 0, \quad r > R. \tag{A.4}$$

I introduce two variables given by

$$k = \sqrt{\frac{M}{\hbar^2}\left(U_0 - E_B\right)}, \quad \kappa = \sqrt{\frac{ME_B}{\hbar^2}}. \tag{A.5}$$

Rewriting equation (A.3) in terms of (A.5) and solving the differential equation yields

$$\frac{\mathrm{d}^2u(r)}{\mathrm{d}r^2} = -ku(r) \Rightarrow u(r) = A\sin(kr) + B\cos(kr). \tag{A.6}$$

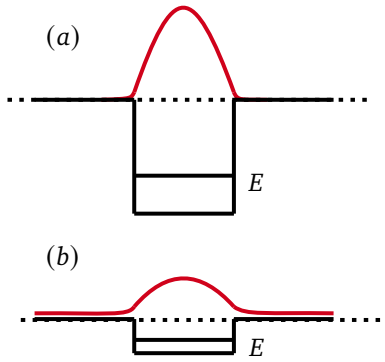

Figure A.1: Behavior of the ground state bound wave function for two potentials. (a) is an illustration of the deeper potential well case and (b) is for a shallower potential well.

Since $R(r) = u(r)/r$ and $\cos(kr)/r$ blows up as $r \to 0 \Rightarrow B = 0$ and the solution is

$$u(r) = A\sin(kr), \quad r \leq R \tag{A.7}$$

Now, considering equation (A.4)

$$\frac{\mathrm{d}^2u(r)}{\mathrm{d}r^2} = \kappa^2 u(r) \Rightarrow u(r) = Ce^{\kappa r} + De^{-\kappa r} \tag{A.8}$$

Here $Ce^{\kappa r}$ blows up as $r \to \infty$. The wavefunction must be continuous and this means the solutions (A.6) and (A.8) must match at $r = R$. The same applies for the derivative. This leads to two equations for $r = R$.

$$A\sin(kR) = De^{-\kappa R} \tag{A.9}$$

$$Ak\cos(kR) = -D\kappa e^{-\kappa R} \tag{A.10}$$

Dividing equation (A.10) by equation (A.9) leads to

$$-\cot(kR) = \frac{\kappa}{k} \tag{A.11}$$

This equation is solved by requiring $kR = \pi/2$. Plugging in an appropiate value for $R = 1.7$ fm yields

$$\begin{aligned} U_0 &= \frac{\hbar^2\pi^2}{2mR^2} - E \\ &= \frac{\hbar^2\pi^2}{2mR^2} + E_B \\ &= 37.2\,\text{MeV} \end{aligned}$$

This means the depth of the potential is 37.2 MeV.

Note that this is all for s-wave. Some considerations about the tensor force are also needed. This means we have to consider the Schrödinger equation with noncentral spin-dependent potential given by

$$\mathcal{U}(r) = \mathcal{U}_0(r) + \mathcal{U}_t(r)S_{12}, \tag{A.12}$$

where

$$\mathcal{U}_t(r) = \mathcal{U}_{tW}(r) + \mathcal{U}_{tM}(r), \tag{A.13}$$

for the space-even states we are considering with the deuteron, see table A. Considering the d-wave I introduce the anglular momentum coupling $[Y_2(\mathbf{n})\chi_1]_{1M}$ of spin 1 and $\ell = 1$ to the total deuteron spin $J = 1$ and projection $J_z = M$. The same coupling but properly normalized can be written as

$$\Theta_M = \frac{1}{\sqrt{32\pi}} S_{12}\chi_{1M}. \tag{A.14}$$

To get the complete wave function of the deuteron the expression must contain two radial parts and a spherical wave factor $1/r$

$$\Psi_M = \frac{1}{\sqrt{4\pi}}\frac{1}{r}\left(u_0(r) + \frac{1}{\sqrt{8}}u_2(r)S_{12}\right)\chi_{1M}, \tag{A.15}$$

where the two radial parts are $u_0(r)$ and $u_2(r)$ for s-wave and d-wave respectivly. These must also be normalized as

$$\int_0^\infty \mathrm{d}r\,|u_0|^2 + \int_0^\infty \mathrm{d}r\,|u_2|^2 = 1, \tag{A.16}$$

and the two terms can be interpreted as a weight for the respective wave. Now using the expression for the deuteron wave function equation

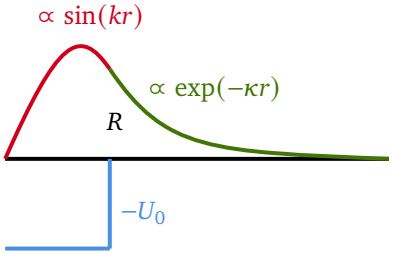

Figure A.2: The s-wave wave function for the deuteron.

	0^+	0^-	1^+	1^-
Singlet	$^1s_0$			$^1p_1$
Triplet		3_0^p	$^3s_1, ^3d_1$	$^3p_1$

Table A.1: Two nucleon states J^Π. The deuteron consists of a wave function superposition of $^3s_1 + ^3d_1$.

(A.15) I want to get an expression for the differential cross section for the nuclear photoeffect. When an absorbed photon frequency is greater than the lowest threshold of nuclear decay the nucleus becomes excited to the continuum states. These states can decay in a number of ways but here are consider the case where the decay happens through particle emission. In other words this is the absorbtion of a photon that results in a particle decay into the continuum. From conservation of energy we have

$$E_i = \hbar\omega = E_f + \epsilon, \tag{A.17}$$

where the nucleus A goes from the inital state with energy E_i to the final state with $A-1$ and energy E_f and the particle in the continuum has energy $\epsilon = \mathbf{p}^2/2m$.

In contrast to the excitation of the discrete states that shows resonance behavior the continuum of energy states makes for a more smooth dependence. This means we can use what we know form the discrete excitation but introduce a level density ρ_f instead of the usual delta function in the expression for the differential cross section. This yields

$$\mathrm{d}\sigma_{fi} = \frac{4\pi^2\hbar}{E_\gamma c}\left|\sum_a \frac{\mathbf{e_a}}{m_a}\left\langle f\right|(\mathbf{p}_a\cdot\mathbf{e}_{\mathbf{k}\lambda})\mathrm{e}^{i(\mathbf{k}\cdot\mathbf{r}_a)}\left|i\right\rangle\right|^2 \rho_f, \tag{A.18}$$

where the level density is given by

$$\rho_f = \frac{Vmp}{(2\pi\hbar)^3}\mathrm{d}o. \tag{A.19}$$

Here the particle is emitted with momentum $\mathbf{p}$ into the solid angle element $\mathrm{d}o$ and E_γ is the energy of the photon. In the case of the deuteron equation (A.18) and be split into different multipolarities and the most simple is the electric dipole transition ($E1$) from the deuteron bound state into the state of continuum motion of the proton and the neutron with reduced mass $m/2$.

In the long wave length limit the plane wave expression reduces to unity which means equation (A.18) for the dipole transition can be written as

$$\mathrm{d}\sigma_{E1} = \frac{\alpha mp\omega}{\hbar^2}\left|\sum_a(\mathbf{e}\cdot\mathbf{r_a})_{fi}\right|^2 \frac{\mathrm{d}o}{4\pi}, \tag{A.20}$$

where the solid angle could be the direction along the motion of the proton[1].

1. Also, $V=1$ and $\alpha = e^2/\hbar c$

When assuming an unpolarized deuteron we can take the average over the spin states $1/3\sum_m$ and count all final polarizations $\sum_{m'}$[2]. The final state is still spin triplet since the dipole operator does not act on the spin variable. This yields

2. Note m and m'

$$\overline{\mathrm{d}\sigma_{E1}} = \frac{1}{4}\frac{\alpha mp\omega}{\hbar^2}\frac{1}{3}\sum_{mm'}\left|(\mathbf{e}\cdot\mathbf{r})_{fi}\right|^2\frac{\mathrm{d}o}{4\pi}. \tag{A.21}$$

The task in now to find an expression for the dot product in the sum. The final spin state after the $E1$ transition remains a triplet with $S=J=1$, the orbital and parity, however, is not the same. The final state corresponds to the p-wave where the low-energy nuclear forces are weak and the wavelength of the relative motion is much larger than the range of those forces. From conservation of energy we have have

$$\frac{\hbar^2k^2}{2m} = \hbar\omega - \epsilon, \tag{A.22}$$

where ϵ is the binding energy of the deuteron also in equation (A.2). For any direction of the relative momentum vector $\hbar\mathbf{k}$ the p-wave component must be normalized through some Legendre polynomial $P_1(\cos(\theta))$ and the spherical Bessel function $j_{\ell=1}(kr)$.[3]

3. $P_1(\cos(\theta)) = \cos(\theta)$ and $j_1(\rho) = \frac{\sin(\rho)-\rho\cos(\rho)}{\rho^2}$.

Here θ is the angle between the relative coordinate $\mathbf{r}$ and the wave vector $\mathbf{k}$ this yields

$$\psi_f(r,\theta) = 3i\cos(\theta)j_1(kr)\chi_{mm'} \tag{A.23}$$

In the s-wave transition we get the following expression when integration over the angles of the unit vector $\mathbf{n} = \mathbf{r}/r$

$$\frac{1}{2}\left\langle f; m'\middle|(\mathbf{e}\cdot\mathbf{r})\middle|\ell = 0; m\right\rangle = -i\frac{\sqrt{\pi}}{k}(\mathbf{e}\cdot\mathbf{k})I_0\delta_{mm'}. \tag{A.24}$$

The radial integrals for the s-wave and d-wave are given by I_0 and I_2 respectively.[4] For the d-wave we have to reintroduce the tensor operator[5] S_12. Just like in the s-wave case we have to integrate over the unit vector – this time, however, it contains four components

4. $I_\ell = \int_0^\infty \mathrm{d}r\, r^2 j_1(kr)u_\ell(r)$, $\ell = 0, 2$

5.

$$S_{12}(\mathbf{n}) = 3(\boldsymbol{\sigma}_1\cdot\mathbf{n})(\boldsymbol{\sigma}_2)\cdot\mathbf{n} - (\boldsymbol{\sigma}_1\cdot\boldsymbol{\sigma}_2) = 2[3(\mathbf{S}\cdot\mathbf{n})^2 - \mathbf{S}^2]$$

$$\int \mathrm{d}o\, n_i n_j n_k n_l = \frac{4\pi}{15}(\delta ij\delta_{kl} + \delta_{ik}\delta_{jl} + \delta_{il}\delta_{jk}), \tag{A.25}$$

and the d-wave contribution is given by

$$\frac{1}{2}\left\langle f; m'\middle|(\mathbf{e}\cdot\mathbf{r})\middle|\ell = 2; m\right\rangle = -i\frac{\sqrt{\pi}}{k}C_{m'm}I_2, \tag{A.26}$$

where the spin matrix element $C_{mm'}$ contains

$$C = \frac{2\sqrt{2}}{5}\left[\frac{3}{4}\left[(\mathbf{k}\cdot\mathbf{S})(\mathbf{e}\cdot\mathbf{S}) + (\mathbf{e}\cdot\mathbf{S})(\mathbf{k}\cdot\mathbf{S})\right] - (\mathbf{e}\cdot\mathbf{k})\right]. \tag{A.27}$$

6.

$$\sum_{mm'}|O_{m'm}|^2 = \sum_m (O^\dagger O)_{mm} = \mathrm{Tr}\{O^\dagger O\}$$

Equation (A.27) can be rewritten using a trace identity[6] Skipping the calculation and moving back to equation (A.21) we have

$$\frac{1}{3}\sum_{mm'}\left|(\mathbf{e}\cdot\mathbf{r})_{fi}\right|^2 = 4\pi\left(I_0^2\cos^2(\alpha) + \frac{1}{25}I_2^2(3+\cos^2(\alpha))\right), \tag{A.28}$$

where α is the angle between $\mathbf{e}$ and the momentum of the final nucleon $\mathbf{k}$. The final steps involve averaging over the transverse polarizations of the initial photon which also relates the angle α to the experimentally observed angle between the directions of the photon and final nucleus. This means we get the following expression

$$\overline{\cos^2(\alpha)} = \frac{1}{2}\sin^2(\theta) \tag{A.29}$$

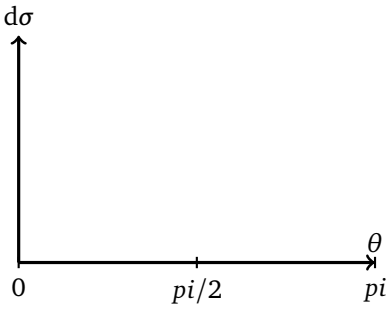

Figure A.3: Behavior of the differential cross section from equation (A.30).

Plugging this into equation (A.20) yields

$$\mathrm{d}\sigma_{E1} = \frac{\pi}{2}\frac{\alpha mp\omega}{\hbar^2}\left[I_0^2\sin^2(\theta) + \frac{1}{25}(6+\sin^2(\theta))I_2^2\right]\frac{\mathrm{d}o}{4\pi}, \tag{A.30}$$

and we arrive at the final expression when integrating over the angle of emitted photons

$$\sigma_{E1} = \frac{\pi}{3}\frac{\alpha mp\omega}{\hbar^2}\left(I_0^2 + \frac{2}{5}I_2^2\right). \tag{A.31}$$

If is also possible to estimate the cross section in equation (A.31) using the initial wave function of the approximation of weak binding. Here the wave function is replaced by its exponential tail outside the range

of nuclear forces. Furthermore, the contribution I_2 is neglected. This means the wave function is given by

$$\psi_i = \sqrt{\frac{\kappa}{2\pi}} \frac{e^{-\kappa r}}{r}, \tag{A.32}$$

where κ is defined in equation (A.5). Calculating the integral I_0 yields

$$\sigma = \frac{8\pi}{3} \frac{\alpha\hbar^2}{M} \frac{\sqrt{\epsilon}(\hbar\omega - \epsilon)^{3/2}}{(\hbar\omega)^3}, \tag{A.33}$$

which is rewritten in terms of the photon energy, $\xi = \hbar\omega/\epsilon$ and in terms of numerical estimates

$$\sigma(\xi) \simeq 1.2 \frac{(\xi - 1)^{3/2}}{\xi^3} \times 10^{-26}\,\mathrm{cm}^2. \tag{A.34}$$

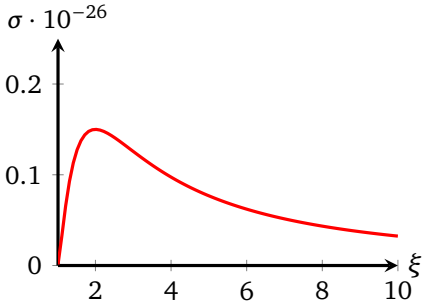

Figure A.4: Behavior of the cross section as a function of photon energy, ξ. Maximum occurs at $0.15 \cdot 10^{-26}$ cm^2 which is equivalent to 1.5 mb.

Appendix **B**

Special functions and properties

In this appendix I wish to cover the basics of some of the special functions that arises when discussing properties of some operators in quantum mechanics. sectionLegendre polynomials

$$Y_\ell^m(\theta,\phi) = \frac{(-1)^{\ell l+m}}{(2\ell)!!}\left[\frac{(2\ell+1)(\ell-m)}{4\pi(\ell+m)!}\right](\sin\theta)^m \frac{\mathrm{d}^{\ell+m}}{(d\cos\theta)^{\ell+m}}[(\sin\theta)^{2\ell}]\exp\{im\phi\}, \tag{B.1}$$

which satisfy

$$Y_\ell^{*m} = (-1)^m Y_l^{-m}. \tag{B.2}$$

The spherical harmonics are connected to the Legendre polynomials

$$P_\ell(\cos\theta) = \left[\frac{4\pi}{2\ell+1}\right]^{1/2} Y_l^0(\theta). \tag{B.3}$$

Another important feature of the spherical harmonics is that they form a complete set of functions over the unit sphere. Furthermore, they form an orthonormal set

$$\int \mathrm{d}\Omega\, Y_\ell^{*m} Y_{l'}^{m'} = \delta_{mm'}\delta_{ll'}. \tag{B.4}$$

Also, there exists an addition theorem for spherical harmonics

$$\sum_{m=-\ell} Y_\ell^{*m}(\theta,\phi) Y_\ell^m(\theta'.\phi') = \left(\frac{2\ell+1}{4\pi}\right)^{1/2} Y_\ell^0(\alpha) \tag{B.5}$$

B.1 Spherical Bessel functions

B.2 Hankel transform

B.3 Coulomb wave functions

Appendix C

Three component wavefunction

Stricly speaking, the nuclear model should be consistent with other results from nuclear physics. In particular, the mass difference between the charged pion and the neutral pion. A prioi we do not know the impact on the wave function of the nucleon-pion system and in this appendix we wish to estimate how the wave function changes when we take the different properties of the pion into account. Starting from (3.13)

$$\psi_p = p \uparrow \frac{1}{\sqrt{V}}, \quad \psi_{N\pi^0} = (\boldsymbol{\tau}\cdot\boldsymbol{\pi})(\boldsymbol{\sigma}\cdot\mathbf{r})\phi_0(r)p \uparrow \frac{1}{\sqrt{V}}, \quad \psi_{N\pi^+} = (\boldsymbol{\tau}\cdot\boldsymbol{\pi})(\boldsymbol{\sigma}\cdot\mathbf{r})\phi_+(r)p \uparrow \frac{1}{\sqrt{V}}, \tag{C.1}$$

and these will act as the state vector in our system. Constructing a similar Hamiltonian for the three component wave function yields

$$\begin{bmatrix} K_{\mathbf{p}} & W^\dagger & W^\dagger \\ W & K_{\mathbf{p}} + K_0 + m_{\pi^0} & 0 \\ W & 0 & K_{\mathbf{p}} + K_+ + m_{\pi^+} \end{bmatrix} \begin{bmatrix} \psi_p \\ \psi_{N\pi^0} \\ \psi_{N\pi^+} \end{bmatrix} = E \begin{bmatrix} \psi_p \\ \psi_{N\pi^0} \\ \psi_{N\pi^+} \end{bmatrix}, \tag{C.2}$$

where K_i is the kinetic operator and W, $W^\dagger$ are the creation and annihilation of a pion respectively. This leads to three coupled equations

$$W^\dagger\psi_{N\pi^0} + W^\dagger\psi_{N\pi^+} = E\psi_p \tag{C.3}$$

$$W\psi_p + (K_0 + m_{\pi^0})\psi_{N\pi^0} = E\psi_{N\pi^0} \tag{C.4}$$

$$W\psi_p + (K_+ + m_{\pi^+})\psi_{N\pi^+} = E\psi_{N\pi^+}. \tag{C.5}$$

The calculations are completely analogous to what is done in chapter 3 and the final set of equations are given by

$$\left.\begin{aligned} &12\pi \int_0^\infty \mathrm{d}r\, f(r)\phi_0(r)r^4 + 12\pi \int_0^\infty \mathrm{d}r\, f(r)\phi_+(r)r^4 = E \\ &f(r) - \frac{\hbar^2}{2\mu_0}\left(\frac{\mathrm{d}^2\phi_0(r)}{\mathrm{d}r^2} + \frac{4}{r}\frac{\mathrm{d}\phi_0(r)}{\mathrm{d}r}\right) + m_\pi^0 c^2\phi_0(r) = E\phi_0(r) \\ &f(r) - \frac{\hbar^2}{2\mu_+}\left(\frac{\mathrm{d}^2\phi_+(r)}{\mathrm{d}r^2} + \frac{4}{r}\frac{\mathrm{d}\phi_+(r)}{\mathrm{d}r}\right) + m_\pi^+ c^2\phi_+(r) = E\phi_+(r) \end{aligned}\right\} \tag{C.6}$$

Physically, we have added another pion wave function to our original model yet it is still bound by the total energy of the system, E. Numerically this almost the same system and the solutions can be found using the same numerical considerations as in section 3.2.1. The results are shown in C.1

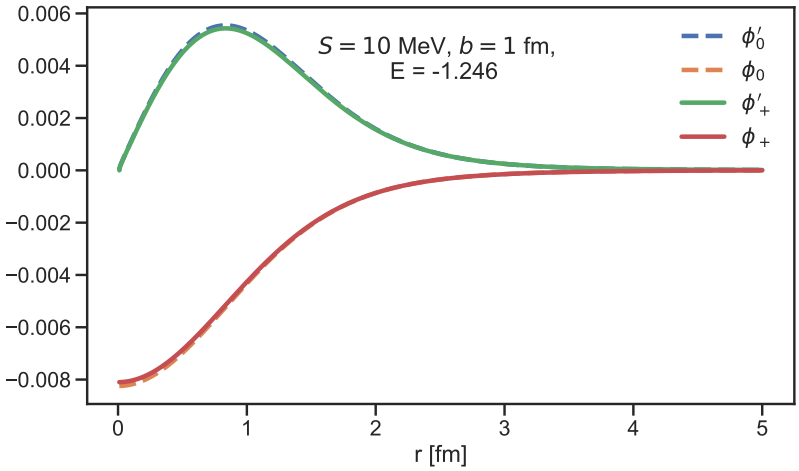

Figure C.1: Solutions to (C.6). The difference in the wave function is minimal compared to the two component wave function. The energy is approximately equal to the sum of the two individual systems.

Compared to 3.4 the difference is negligible even accounting for the mass difference for the pions and nucleons (m_N, m_P). This means we can to a good estimation continue using only one pion wave function in our nuclear model.

Bibliography

Beck, R., Kalleicher, F., Schoch, B., Vogt, J., Koch, G., Ströher, H., Metag, V., McGeorge, J. C., Kellie, J. D., and Hall, S. J. (1990). Measurement of the p(γ,π^0) cross section at threshold. *Phys. Rev. Lett.*, 65:1841–1844.

Fedorov, D. V. (2020). A nuclear model with explicit mesons. *Few-Body Systems*, 61(4).

Schmidt, A., Achenbach, P., Ahrens, J., Arends, H. J., Beck, R., Bernstein, A. M., Hejny, V., Kotulla, M., Krusche, B., Kuhr, V., Leukel, R., MacGregor, I. J. D., McGeorge, J. C., Metag, V., Olmos de León, V. M., Rambo, F., Siodlaczek, U., Ströher, H., Walcher, T., Weiß, J., Wissmann, F., and Wolf, M. (2001). Test of low-energy theorems for ${}^1h(\vec{\gamma},\pi^0){}^1h$ in the threshold region. *Phys. Rev. Lett.*, 87:232501.

Zelevinsky, V. and Volya, A. (2017). *Physics of Atomic Nuclei*. Wiley-VCH, first edition.